



Hohenpeissenberg Photochemical Experiment (HOPE 2000): Measurements and photostationary state calculations of OH and peroxy radicals

G. M. Handisides, C. Plass-Dülmer, S. Gilge, H. Bingemer, H. Berresheim

► To cite this version:

G. M. Handisides, C. Plass-Dülmer, S. Gilge, H. Bingemer, H. Berresheim. Hohenpeissenberg Photochemical Experiment (HOPE 2000): Measurements and photostationary state calculations of OH and peroxy radicals. *Atmospheric Chemistry and Physics Discussions*, 2002, 2 (6), pp.2507-2555.
hal-00301026

HAL Id: hal-00301026

<https://hal.science/hal-00301026>

Submitted on 18 Jun 2008

HAL is a multi-disciplinary open access archive for the deposit and dissemination of scientific research documents, whether they are published or not. The documents may come from teaching and research institutions in France or abroad, or from public or private research centers.

L'archive ouverte pluridisciplinaire **HAL**, est destinée au dépôt et à la diffusion de documents scientifiques de niveau recherche, publiés ou non, émanant des établissements d'enseignement et de recherche français ou étrangers, des laboratoires publics ou privés.



Hohenpeissenberg Photochemical Experiment (HOPE 2000): Measurements and photostationary state calculations of OH and peroxy radicals

G. M. Handisides¹, C. Plass-Dülmer², S. Gilge², H. Bingemer¹, and H. Berresheim²

¹Institute for Meteorology and Geophysics, Frankfurt am Main, Germany

²German Weather Service, Hohenpeissenberg, Germany

Received: 31 October 2002 – Accepted: 26 November 2002 – Published: 18 December 2002

Correspondence to: G. M. Handisides (handisides@mete.or.uni-frankfurt.de)

Hohenpeissenberg
Photochemistry
Experiment

Handisides et al.

[Title Page](#)

[Abstract](#)

[Introduction](#)

[Conclusions](#)

[References](#)

[Tables](#)

[Figures](#)

◀

▶

◀

▶

[Back](#)

[Close](#)

[Full Screen / Esc](#)

[Print Version](#)

[Interactive Discussion](#)

© EGU 2002

Abstract

ACPD

2, 2507–2555, 2002

Measurements of OH, the sum of peroxy radicals (RO_x), non-methane hydrocarbons (NMHCs) and various other trace gases were made at the Meteorological Observatory Hohenpeissenberg in June 2000. The data from an intensive measurement period characterised by high solar insolation (18–21 June) are analysed. The maximum midday OH concentration ranged between 4.5×10^6 molecules cm^{-3} and 7.4×10^6 molecules cm^{-3} . The maximum total RO_x mixing ratio increased from about 55 pptv on 18 June to nearly 70 pptv on 20 and 21 June. A total of 64 NMHCs, including isoprene and monoterpenes, were measured every 1 to 6 hours. The oxidation rate of the NMHCs by OH was calculated and reached a total of over 14×10^6 molecules $\text{cm}^{-3} \text{s}^{-1}$ on two days. A simple photostationary state balance model was used to simulate the ambient OH and RO_x concentrations with the measured data as input. The model was able to reproduce the main features of the diurnal profiles of both OH and RO_x . The model results proved to be most sensitive to assumptions about the mixing ratio of formaldehyde (HCHO), which was included as a proxy for carbonyl compounds, and about the partitioning between HO_2 and RO_2 . The measured OH concentration and RO_x mixing ratios were reproduced well by assuming the presence of 3 ppbv HCHO and a HO_2/RO_2 ratio between 1:1 and 1:2. The most important source of OH, and conversely the greatest sink for RO_x , was the recycling of HO_2 radicals to OH. This reaction was responsible for the recycling of more than 45×10^6 molecules $\text{cm}^{-3} \text{s}^{-1}$ on two days. The most important sink for OH, and the largest source of RO_x , was the oxidation of NMHCs, in particular, of isoprene and the monoterpenes.

1. Introduction

Free radicals play an important role in the chemical self-cleansing of the atmosphere. The hydroxyl radical, OH, is the main oxidising agent during daytime for many volatile organic compounds (VOCs), and other trace gases. Peroxy radicals ($\text{RO}_x = \text{RO}_2 + \text{HO}_2$,

Hohenpeissenberg
Photochemistry
Experiment

Handsides et al.

[Title Page](#)

[Abstract](#)

[Introduction](#)

[Conclusions](#)

[References](#)

[Tables](#)

[Figures](#)

◀

▶

◀

▶

[Back](#)

[Close](#)

[Full Screen / Esc](#)

[Print Version](#)

[Interactive Discussion](#)

© EGU 2002

where R represents an organic group) are produced during many of these oxidation reactions. These peroxy radicals can react with NO to produce NO₂, which leads to the production of ozone in the troposphere if the mixing ratio of NO exceeds 10–30 pptv (Atkinson, 2000).

- 5 The primary source of OH radicals in the troposphere is the photolysis of ozone and the subsequent reaction of the resulting O(¹D) with water vapour:



The OH radicals react with a large number of trace gases, including CH₄, CO and non-methane hydrocarbons (NHMCs). These reactions typically result in the production of peroxy radicals:



Carbonyl compounds, e.g. HCHO and CH₃CHO, can be a significant source of peroxy radicals (e.g. Poppe et al., 1994; Carslaw et al., 2002) via photolysis and oxidation by OH, e.g. for HCHO:



and by the conversion of the H atom generated in Reaction 7 following Reaction 4.

A further source of peroxy radicals is the oxidation of alkenes by the nitrate radical, NO₃, and a small yield from the oxidation of alkenes by ozone. In the presence of

Hohenpeissenberg Photochemistry Experiment

Handisides et al.

[Title Page](#)

[Abstract](#)

[Introduction](#)

[Conclusions](#)

[References](#)

[Tables](#)

[Figures](#)

◀

▶

◀

▶

[Back](#)

[Close](#)

[Full Screen / Esc](#)

[Print Version](#)

[Interactive Discussion](#)

high mixing ratios of biogenic alkenes, these reactions can be significant, although the reaction involving the NO_3 radical is only of importance at night, as NO_3 is rapidly photolysed during daytime.

The most important sink for RO_2 radicals is the reaction with NO:



10 where $\text{R}'\text{O}$ in Reaction 11 is a carbonyl compound and R' is equal to R except for the loss of one H atom. Reaction 12 represents an important secondary source of OH via recycling.

15 A number of combined field and modeling investigations of the HO_X ($\text{HO}_X = \text{OH} + \text{HO}_2$) radical budget and of ozone formation have been undertaken to test our current understanding of photochemistry (e.g. [Carslaw et al., 2001](#)). In particular, concurrent measurements of both OH and HO_2 have been made by several groups using the LIF method (e.g. [Creasey et al., 2002](#); [Tan et al., 2001](#); [Abram et al., 2000](#); [George et al., 1999](#)). However, only a few campaigns have been reported in which measurements of both OH and RO_X radicals were made (e.g. [Carslaw et al., 2002](#); [Platt et al., 2002](#); 20 [Carslaw et al., 1999](#)) and only two of these were made in rural background environments.

The Tropospheric OH Photochemistry Experiment (TOHPE) took place in the Rocky Mountains and included a broad range of measurement parameters, in particular OH ([Tanner et al., 1997](#); [Mount et al., 1997](#); [Mather et al., 1997](#)), HO_2 ([Mather et al., 1997](#)) and RO_X ([Cantrell et al., 1997a](#)). OH and HO_2 concentrations were overestimated using a photostationary state model by 50% and by a factor of about 4, respectively ([McKeen et al., 1997](#)). Proxy assumptions for hydrocarbon species with reactivities

Hohenpeissenberg Photochemistry Experiment

Handisides et al.

[Title Page](#)

[Abstract](#)

[Introduction](#)

[Conclusions](#)

[References](#)

[Tables](#)

[Figures](#)

◀

▶

◀

▶

[Back](#)

[Close](#)

[Full Screen / Esc](#)

[Print Version](#)

[Interactive Discussion](#)

and mixing ratios similar to β -pinene led to an improvement in the agreement between model results and measurements for both radical species.

The Program for Research on Oxidants: Photochemistry, Emissions and Transport (PROPHET) took place at a forested site in northern Michigan (Carroll et al., 2001).

5 OH and HO_2 measurements (Tan et al., 2001) were made in air characterised by high levels of isoprene and other biogenic hydrocarbons and low levels of NO and NO_2 . Model results using a tightly constrained photochemical point model underestimated OH by a factor of 2.7, but were in good agreement with measured HO_2 .

Model results have tended to overestimate the OH concentration (Carslaw et al., 10 2002, 1999; George et al., 1999), with the PROPHET campaign representing a significant exception. Constraining the HO_2 or RO_x concentration using measured values tends to result in much better agreement between model results and measurements (e.g. George et al., 1999).

The aim of the Hohenpeissenberg Photochemistry Experiment (HOPE 2000) was to 15 test our current understanding of free radical photochemistry in a rural environment using a photostationary radical balance model on the basis of measurements of both OH and RO_x . This allowed the model to be constrained by measured radical concentrations. The short lifetimes of free radicals allow the use of a relatively simple box model, without having to consider transport processes. The data set for the model consists of 20 measurements of OH, the sum of peroxy radicals (RO_x), and with an extensive range of NMHCs and other trace gases relevant to OH and RO_x chemistry. These were contributed by the Global Atmosphere Watch (WMO/GAW) monitoring programme at Hohenpeissenberg. Measurements of carbonyl compounds were not made during the HOPE 2000 campaign. However, the contributions of carbonyl compounds were considered and taken into account during the radical balance calculations.

Hohenpeissenberg Photochemistry Experiment

Handsides et al.

[Title Page](#)

[Abstract](#)

[Introduction](#)

[Conclusions](#)

[References](#)

[Tables](#)

[Figures](#)

◀

▶

◀

▶

[Back](#)

[Close](#)

[Full Screen / Esc](#)

[Print Version](#)

[Interactive Discussion](#)

2. Experiment

The Hohenpeissenberg Photochemistry Experiment (HOPE 2000) was conducted between 18 June and 6 July, 2000 at the Meteorological Observatory Hohenpeissenberg. The observatory is both a meteorological monitoring and a Global Atmosphere Watch site operated by the German Weather Service (DWD). It is located in a rural agricultural and forested area approximately 40 km from the northern rim of the Alps at 980 m a.s.l. (47°48' N, 11°02' E, see Fig. 1), and about 300–400 m above the surrounding countryside. There are no significant industrial sources in the vicinity. The nearest city, Munich, is approximately 70 km to the northeast of the site.

The initial four day period of the campaign (18 to 21 June) was characterised by fine weather conditions, relatively high daytime temperatures (up to 27°C) and intense photochemical activity associated with a high pressure system over central Europe. The wind was generally from the east during daytime, with relatively light winds of under 4 m s⁻¹. This episode was the focus of an intensive series of measurements presented here.

The inlets for all trace gas monitoring instruments were located in close proximity to each other on the roof of a container tower at approximately 10 m above ground level, which is the height of the nearby trees. Meteorological measurements were made at a horizontal distance of 50 m from the container tower. Wind measurements were made on top of a 40 m mast.

The instrumentation used during HOPE, with the exception of the standard meteorological instrumentation, is summarised in Table 1.

Atmospheric OH concentrations were measured using the selected ion/chemical ionisation mass spectrometry (SI/CIMS) technique as described by Berresheim et al. (2000). The measurement principle is based on three major steps: (1) Titration of the OH in the sample air by excess ³⁴SO₂ to produce the heavy isotope H₂³⁴SO₄, (2) Charge transfer of the H₂³⁴SO₄ with NO₃⁻ ions (which are selectively formed in a separate purified air flow by alpha bombardment from a radioactive ²⁴¹Am source) resulting

Hohenpeissenberg Photochemistry Experiment

Handsides et al.

[Title Page](#)

[Abstract](#)

[Introduction](#)

[Conclusions](#)

[References](#)

[Tables](#)

[Figures](#)

◀

▶

◀

▶

[Back](#)

[Close](#)

[Full Screen / Esc](#)

[Print Version](#)

[Interactive Discussion](#)

© EGU 2002

**Hohenpeissenberg
Photochemistry
Experiment**

Handisides et al.

in $\text{H}^{34}\text{SO}_4^-$ product ions, and (3) Measurement of the $\text{H}^{34}\text{SO}_4^-/\text{NO}_3^-$ ion ratio by MS after transfer of the ions into the vacuum region. To measure the background signal, excess high purity propane is added to the sample air/ SO_2 mixture to scavenge the OH radicals by reaction with the propane instead of SO_2 . The OH concentration is determined from the $\text{H}^{34}\text{SO}_4^-/\text{NO}_3^-$ signal ratio using a calibration factor, F, which is determined each day. Calibration is based on UV-photolysis ($\lambda=185\text{ nm}$) of ambient air water vapour in front of the sample tube. This yields OH concentrations in the $10^7\text{--}10^8$ molecule cm^{-3} range. The OH concentration is calculated based on the known H_2O absorption cross section (Cantrell et al., 1997b), concurrent measurements of $[\text{H}_2\text{O}]$ using a chilled mirror dewpoint hygrometer (Michell Instruments), and the photon flux in the photolysis zone, which is measured using calibrated (solar-blind) photocathodes (Hamamatsu).

OH concentrations measured during the HOPE campaign were corrected for errors resulting from chemical reactions within the measurement system. The correction followed an iterative chemical model previously described by Berresheim et al. (2000) and Tanner et al. (1997). Corresponding corrections were calculated for chemical reactions in both the sample inlet and the OH titration zone using measured ambient air concentrations of NO, NO_2 , CO and NMHCs. Depending on the concentrations of these compounds, the resulting total corrections ranged from 15% to 35%. Taking these corrections into account, the overall 2σ precision, accuracy, and detection limit of the OH measurements with 5 minute signal integration during the HOPE campaign were 31%, 39%, and 4×10^5 molecule cm^{-3} , respectively.

The mixing ratio of the peroxy radicals (RO_x) was measured using a peroxy radical chemical amplifier (CA) built by Handisides (2001). The peroxy radical chemical amplifier technique (Cantrell et al., 1984; Hastie et al., 1991) has been used in a large number of campaigns (Platt et al., 2002; Carslaw et al., 2002; Monks et al., 1996; Cantrell et al., 1996, e.g.). In a recent field campaign (Platt et al., 2002), it was shown to compare well with direct RO_x measurements made using Matrix Isolation/Electron Spin Resonance (MIESR) (Mihelcic et al., 1990). The design of the instrument used in

[Title Page](#)[Abstract](#)[Introduction](#)[Conclusions](#)[References](#)[Tables](#)[Figures](#)[◀](#)[▶](#)[◀](#)[▶](#)[Back](#)[Close](#)[Full Screen / Esc](#)[Print Version](#)[Interactive Discussion](#)

**Hohenpeissenberg
Photochemistry
Experiment**

Handisides et al.

HOPE 2000 is essentially identical to that of the instrument described by [Hastie et al. \(1991\)](#). The technique relies on a chain reaction between peroxy radicals and added NO and CO, in which NO is oxidised to NO₂. The chain reaction results in the production of n molecules of NO₂ for each peroxy radical, where n is the length of the chain reaction and represents the signal amplification. During HOPE 2000, the value of n obtained by calibration in dry air exceeded 160. The reaction product NO₂ is subsequently detected via its reaction with luminol using a liquid phase chemiluminescence detector. The amplification is modulated to allow the effect of ambient NO₂ to be accounted for ([Hastie et al., 1991](#), see). PFA Teflon tubing with 6.35 mm (1/4") o.d. and 4.83 mm (0.190") i.d. was used for the intake and all subsequent tubing in contact with the air sample. The distance between the addition points for CO was 1.6 m and the length of tubing between the second downflow addition point and the NO₂ detector was 10 m. The flow rate of ambient air through the system was 1.61 l min⁻¹. Radical calibration was performed using the photolysis of water at 185 nm generated by a PenRay mercury lamp ([Schultz et al., 1995](#)).

The CA technique has been found to be sensitive to the relative humidity in the sample air ([Mihele and Hastie, 1998](#); [Mihele et al., 1999](#); [Mihele and Hastie, 2000](#); [Reichert, 2000](#)). The CA measurements were corrected for this effect using a parameterisation of the data of [Mihele and Hastie \(2000\)](#), which were obtained using a similar Teflon inlet to that of the CA used here. The accuracy of the measurements is about $\pm 60\%$ at 50% relative humidity and is better when the air is drier. The data from the HOPE 2000 campaign presented here were measured at relative humidities between 25 and 50%. The average 2- σ detection limit was about 6 pptv at nighttime and increased to 9 pptv during the day.

Ambient C₂-C₁₀ NMHC mixing ratios were measured online using two GC-systems operating simultaneously. During the period from 17 to 20 June, measurements of 64 species (see Table 3) were made every one to three hours during daytime. Both GCs share a common intake system in which ambient air is continuously flushed through a 10 m long, 4 cm i.d. glass tube (Duran®, Schott Glaswerke, Mainz, Germany) at a flow

Title Page	
Abstract	Introduction
Conclusions	References
Tables	Figures
◀	▶
◀	▶
Back	Close
Full Screen / Esc	
Print Version	
Interactive Discussion	

rate of $1 \text{ m}^3 \text{ min}^{-1}$ using a fan installed at the downstream end of the tube. Samples were transferred to each GC system from the centre of the air inlet flow through a silica-lined stainless steel tube (1 m, 1/8" o. d., SILCOSTEEL, Restek Corp., Bellefonte, PA, USA).

- 5 The first GC system (GC-1, Varian 3600 CX) is used to detect light NMHCs ($\text{C}_2\text{-C}_8$) and is described in detail in [Plass-Dülmer et al. \(2002\)](#). Ambient air samples (typically 750 cm^3) are passed through heated stainless steel tubes serving as an effective ozone trap and a Nafion dryer for water vapour removal before the NMHC compounds are cryogenically trapped on glass beads cooled to 85 K. After cryotrapping, the sample is desorbed at 473 K onto an $\text{Al}_2\text{O}_3/\text{KCl}$ GC column (50 m, 0.53 mm i.d.). Following chromatographic separation, the individual compounds are detected by a flame ionisation detector (FID).
- 10

The second system (GC-2, Varian 3400CX) is optimised for the detection of $\text{C}_5\text{-C}_{13}$ NMHCs including isoprene and monoterpenes, and is similar to systems that have been successfully used by other groups for measuring these compounds ([Helming et al., 1998](#); [Riemer et al., 1994](#); [Goldan et al., 1995](#)). Its main components are an ozone scrubber, an adsorption trap, a cryo-focussing unit, a gas chromatograph and a FID/MS detector. An air sample is taken from the main intake line at a flow rate of 50-80 ml min^{-1} and passes through a glass fibre filter impregnated with $\text{Na}_2\text{O}_3\text{S}_2$ to remove ozone ([Helming et al., 1998](#)). In a sample preconcentration trap (1/8" o.d. and 30 cm length, SPT, Varian Inc.) NMHCs are adsorbed onto Carbopack B (40/60 mesh, Supelco Inc.) at 303 K. The sample is desorbed at 503 K in a helium carrier gas flow of 30 ml min^{-1} , and re-focussed again at 77 K in a silcosteel capillary (0.28 mm i.d., 20 cm). After desorption at 453 K, NMHC are injected onto a BPX-5 column (50 m, 0.22 mm i.d.) in a helium carrier gas flow of 1.8 ml min^{-1} . All materials in contact with the sample gas flow have inert surfaces, e.g. silcosteel, fused silica, and PTFE, and the Valco multiport valves (423 K, VICI CH) are made of stainless steel and Valcon-E. Chromatographic separation is achieved by using a temperature programme with an initial isothermal phase (283 K, 10 min) followed by a temperature ramp of 6 K/min to

Hohenpeissenberg Photochemistry Experiment

Handsides et al.

[Title Page](#)

[Abstract](#)

[Introduction](#)

[Conclusions](#)

[References](#)

[Tables](#)

[Figures](#)

◀

▶

◀

▶

[Back](#)

[Close](#)

[Full Screen / Esc](#)

[Print Version](#)

[Interactive Discussion](#)

© EGU 2002

Hohenpeissenberg Photochemistry Experiment

Handsides et al.

[Title Page](#)

[Abstract](#)

[Introduction](#)

[Conclusions](#)

[References](#)

[Tables](#)

[Figures](#)

◀

▶

◀

▶

[Back](#)

[Close](#)

[Full Screen / Esc](#)

[Print Version](#)

[Interactive Discussion](#)

© EGU 2002

511 K. The column effluent is split to an FID and an ion trap mass spectrometer (ITMS, Varian) at a fixed ratio of approximately 4:1. Quantification is based on the integration of selected mass peaks of characteristic fragment ions such as $m/z = 136$ for some of the terpene compounds, and measurements of different calibration gas mixtures on a regular basis.

A detailed quality assurance and quality control procedure has been developed for GC-2 similar to that described by Plass-Dülmer et al. (2002) for the measurements of light NMHC. It includes a thorough characterisation and optimisation of the system combined with frequent checks of the system's performance by measurements of 5 standards, reference gases and zero gas. The monoterpenes are the most difficult of the C_5 - C_{13} NMHCs to measure for the following reasons: (1) they are highly reactive towards other constituents of air, especially ozone, (2) they may be subject to rearrangement reactions during concentration and thermal desorption, and (3) compounds with relatively low vapor pressures, e.g. 1,8-cineol, may partially be lost by 10 adsorption on surfaces. The GC system used during the HOPE campaign has been thoroughly tested by direct measurements of individual monoterpenes and a terpene mixture (12 different monoterpenes at approximately 10 ppbv in N_2), and by standard addition measurements. The latter involved adding a small amount of an individual terpene or a terpene mixture to ambient air just in front of the silcosteel sample line. 15 Artefacts arising from the various error sources outlined above were observed for several terpenes, however, they did not generally exceed 30% (see the corresponding accuracies in Table 3). Sabinene showed substantial decomposition and its measurement was estimated to have an uncertainty of 60%. Products of the decomposition of sabinene in the analytical system were identified as p-cymene, α - and γ -terpinene. For 20 this reason, and due to their low concentrations, the measurements of ambient α - and γ -terpinene were considered to have an uncertainty of 100% and 50%, respectively. Consequently, α -terpinene data were discarded from the HOPE 2000 data set. Overall, the accuracies (2σ) of most of the analysed NMHCs are better than 20% or a few pptv (Table 3). Detection limits are generally less than 10 pptv, and for the majority of 25

compounds lie below 1–3 pptv.

3. Measurement Results

The results from the measurements during the intensive phase, 18 to 21 June, 2000, are presented in Figs. 2 to 4. The OH concentrations and the mixing ratios of RO_X, ozone, NO, NO₂, H₂O₂, ROOH, CO and SO₂ are shown in Fig. 2. Figure 3 shows the most important meteorological parameters for the same time interval. The mixing ratios of the most relevant NMHCs or groups of NMHCs are shown in Fig. 4. The maximum daily temperature exceeded 25°C on each day except for 18 June. Clear skies associated with synoptic high pressure conditions resulted in intense insolation and strong photochemical activity on each of the four days. Consequently, the profiles of O₃, RO_X, OH, NO, isoprene and the terpenes all exhibit a strong diurnal behaviour. At nighttime, the station was situated above the boundary layer, so that ozone mixing ratios typically remained above 50 ppbv, and NO₂ mixing ratios below 2 ppbv.

The diurnal profiles of several trace gases provided evidence of significant vertical air mass transport between about 8:00 and 11:00 CET on each of the four days considered. During these events, air arriving at the measurement site due to convective lifting of the boundary layer was enriched in a number of trace gases with surface sources. This occurred most obviously on June 19 and 20, as shown by the corresponding mixing ratios of NO and NO₂, some of the NMHCs, especially the biogenic terpenes and isoprene, and – to a lesser extent – of CO and SO₂. A corresponding dip in the O₃ mixing ratio can be attributed to titration of O₃ at the elevated NO mixing ratios and to O₃ deposition. This interpretation is further supported by a corresponding increase in relative humidity on most days and the minimum in horizontal wind velocities on all days except 21 June (see Fig. 3).

During some evenings, peaks in the mixing ratios of several trace gases were observed in conjunction with changes in wind speed and direction. These represent a deviation from their respective diurnal profiles and suggest that large scale advection

Hohenpeissenberg Photochemistry Experiment

Handsides et al.

[Title Page](#)

[Abstract](#)

[Introduction](#)

[Conclusions](#)

[References](#)

[Tables](#)

[Figures](#)

◀

▶

◀

▶

[Back](#)

[Close](#)

[Full Screen / Esc](#)

[Print Version](#)

[Interactive Discussion](#)

© EGU 2002

of polluted air masses occurred after sunset. The mixing ratios of O₃, SO₂, CO and NO₂ all showed pronounced peaks between about 18:00 and 22:00 CET. The O₃ mixing ratios always increased first, and dropped again later at the same time as the NO₂ mixing ratio increased.

- 5 The OH concentration reached a maximum between 09:00 and 12:00 CET and generally dropped to below the detection limit of $4 \times 10^5 \text{ cm}^{-3}$ after 19:00–20:00 CET in the evening. On 19 and 20 June, OH reached maximum daytime concentrations of $7 - 8 \times 10^6 \text{ cm}^{-3}$. As can be seen in the upper panel of Fig. 2, the shape of the diurnal profile of the OH concentration was similar to that of j_{O₁D} in the early morning and late
10 afternoon on all days. However, the two profiles deviated considerably around local midday.

- Maximum RO_X mixing ratios occurred at around 14:00 CET and rose from about 55 pptv on the 18th to around 70 pptv on both 20 and 21 June (Fig. 2). Levels of up to 10 pptv RO_X were observed at night, and were probably caused by enhanced
15 night-time oxidation of NMHC by the nitrate radical and by O₃, and the slow loss rate of the peroxy radicals in the absence of NO. The reaction rate with NO₃ and O₃ is much faster for secondary alkenes, such as isoprene and the terpenes, than for other alkenes and other NMHCs (Atkinson, 1997). Although no NO₃ measurements were available, alkene measurements showed that concentrations of a few pptv to 150 pptv
20 of individual biogenic NMHCs were present at night, particularly of isoprene. Mixing ratios for the sum of all measured anthropogenic alkenes reached nearly 500 pptv during the early morning on 19 and 21 June. This may have allowed significant RO_X production by night-time oxidation.

- The profiles of various groups of NMHCs are shown in Fig. 4. The upper panel shows
25 the total concentrations for three groups of NMHCs which are predominantly anthropogenic in origin: alkenes (not including isoprene or terpenes), aromatic compounds, and a group including both alkanes and alkynes. The profiles of isoprene and various measured terpenes are shown in the lower panel. These exhibit marked diurnal variations consistent with their strong biogenic emission sources. The biogenic emis-

Hohenpeissenberg Photochemistry Experiment

Handsides et al.

[Title Page](#)

[Abstract](#)

[Introduction](#)

[Conclusions](#)

[References](#)

[Tables](#)

[Figures](#)

◀

▶

◀

▶

[Back](#)

[Close](#)

[Full Screen / Esc](#)

[Print Version](#)

[Interactive Discussion](#)

© EGU 2002

sions of isoprene increase with light intensity and temperature, whereas emissions of monoterpenes are only dependent on temperature (Guenther et al., 1993). This results in a maximum mixing ratio of up to 600 pptv around noon for isoprene, and a broad maximum in the afternoon for the monoterpenes, e.g. of up to 200 pptv for α -pinene.

5 The nighttime mixing ratios of terpenes decreased to below 20 pptv because the nighttime biogenic emissions mostly took place within the boundary layer. The breakup of the nocturnal inversion layer in the morning led to a peak in the terpene mixing ratios between 8:00 and 11:00 CET.

OH oxidation rates were calculated for individual NMHCs on the basis of the OH and
10 NMHC measurements and the corresponding rate coefficients as listed in Table 3. The resulting total NMHC oxidation rate due to OH is plotted in Fig. 5, along with the individual rates for isoprene and the terpenes. As is to be expected from the OH profile, the highest oxidation rate occurred during morning and around noon, between approximately 09:00 and 13:00 CET. The highest conversion rate for an individual compound
15 was observed for isoprene, and reached over 7×10^6 molecules $\text{cm}^{-3} \text{ s}^{-1}$ on 20 June. The total oxidation rate of the sum of all monoterpenes was also relatively high, and was equal or greater than the total conversion rate of all other NMHCs taken together.

Although no NO_3 measurements were available, it can be assumed that NO_3 radical concentrations built up after sunset from the reaction of NO_2 with ozone. The
20 NMHC data show evidence for the presence of NO_3 radicals, since the rapid decline after 18:00 CET of those biogenic VOC which are less reactive towards ozone, e.g. isoprene, β -pinene, camphene and 3-carene, cannot be explained by OH and ozone chemistry alone. Consequently, it is likely that RO_x production from NO_3 -alkene reactions contributed to the observed nighttime RO_x levels.

Hohenpeissenberg Photochemistry Experiment

Handisides et al.

[Title Page](#)

[Abstract](#)

[Introduction](#)

[Conclusions](#)

[References](#)

[Tables](#)

[Figures](#)

◀

▶

◀

▶

[Back](#)

[Close](#)

[Full Screen / Esc](#)

[Print Version](#)

[Interactive Discussion](#)

4. Discussion

4.1. Photostationary state radical balance model

In order to investigate the consistency of the measurements and our current understanding of atmospheric radical chemistry, the concentrations of OH and RO_X were calculated using a simple photostationary state model. The measured data from 18-21 June were used as model input parameters. Photostationary state conditions were assumed for each of the radical species under consideration, i.e. both OH and RO_X were assumed to be sufficiently short-lived that they remain in steady state with the ambient conditions. Under photostationary state conditions, the production and loss rates for each of the radicals are assumed to be equal.

$$\frac{d[X]}{dt} \approx 0 = P_X - L_X \quad (15)$$

where P_X represents the total production rate for radical X, and L_X is the corresponding loss rate. The set of equations describing the balance between production and loss rates can then be solved for the radical under consideration, and the concentration of that species can be calculated. The concentrations of all measured trace gases other than the specific radical under consideration were used as input for the calculations. Figure 6 is a block diagram showing the chemical interactions included in the model.

The corresponding radical concentration was calculated for the times for which measured NMHC data were available. The results of the model calculations are compared with the measurements and discussed in the following section. The reactions and rate coefficients included in the radical balance calculations are listed in Table 2. The rate coefficients for the oxidation of individual hydrocarbon species by OH are listed in Table 3. The primary production rate of OH (denoted P(OH), No. 1 in Table 2) was calculated using measured ambient O₃ and H₂O concentrations and the measured photolysis rate of O₃, j_{O¹D}. The photolysis rates for H₂O₂ and HCHO were calculated using the System for Transfer of Atmospheric Radiation (STAR) transfer model devel-

Hohenpeissenberg Photochemistry Experiment

Handsides et al.

[Title Page](#)

[Abstract](#)

[Introduction](#)

[Conclusions](#)

[References](#)

[Tables](#)

[Figures](#)

◀

▶

◀

▶

[Back](#)

[Close](#)

[Full Screen / Esc](#)

[Print Version](#)

[Interactive Discussion](#)

© EGU 2002

oped by Ruggaber et al. (1994) and further modified by Schwander et al. (2001). OH production due to the reaction of alkenes with ozone was calculated using the corresponding radical yields compiled by Atkinson (1997).

To solve the equations exactly, the identity and concentration of each of the various organic peroxy radicals present in the air sample would have to be known. Since such detailed measurements are not possible with currently available techniques, a set of assumptions about the chemical behaviour and composition of the peroxy radicals were made and a basic scenario for the calculations was established. The effects of these assumptions on the model results will be discussed in Sect. 4.4.

In the base case scenario, the model was simplified by assuming that HO_2 and CH_3O_2 were the only peroxy radicals present, and that they were present in equal concentrations.

$$[\text{HO}_2] = [\text{RO}_2] = 0.5[\text{RO}_x]_{\text{measured}} \quad (16)$$

Measurements by Mihelcic et al. (1993) and Mihelcic et al. (2001) have shown that for daytime conditions, HO_2 and RO_2 are often present in nearly equal amounts in the continental atmosphere. As the concentration of OH is typically two orders of magnitude less than that of HO_2 , the contribution of OH to the measured RO_x concentration is negligible. It is to be expected that CH_3O_2 constitutes a significant fraction of the organic radicals, as it is a product of the oxidation chains for most hydrocarbon species. Consequently, the reaction rates for the methyl peroxy radical, $\text{CH}_3\text{O}_2(k_{14a}, k_{16a})$ were used for reactions involving RO_2 .

The production of RO_X radicals via the oxidation of NMHCs by O_3 was not included in the base run. Ozonolysis of biogenic alkenes may lead to RO_X production (Atkinson, 1997), particularly at the high concentrations of both ozone and biogenic alkenes present during the day (see Figs. 2 and 4). However, the available kinetic data on NMHC ozonolysis does not readily allow the yields of HO_2 or RO_2 to be calculated. Using the Master Chemical Mechanism (MCM), Carslaw et al. (2002) found that this source of RO_X made only a minor contribution to the total RO_X production (see also Sect. 4.4).

Hohenpeissenberg Photochemistry Experiment

Handsides et al.

[Title Page](#)

[Abstract](#)

[Introduction](#)

[Conclusions](#)

[References](#)

[Tables](#)

[Figures](#)

◀

▶

◀

▶

[Back](#)

[Close](#)

[Full Screen / Esc](#)

[Print Version](#)

[Interactive Discussion](#)

Measured concentrations were used for all trace gases in the model except for HCHO, CH₄ and H₂, which were not measured. The concentration of CH₄ was approximated using the average value of 1.842 ppmv for June 2002 measured at the UBA station at Schauinsland in Southern Germany ([Umweltbundesamt, 2001](#)). A H₂ concentration of 500 ppbv, which is typical for the Northern Hemisphere ([Novelli et al., 1999](#)), was used to approximate the H₂ concentration. A constant mixing ratio of 3 ppbv was assumed for formaldehyde, HCHO, as a proxy for the oxygenated NMHCs. This assumption seems to be reasonable based on the concentrations of formaldehyde, acetaldehyde, acetone, methylvinylketone, and methacrolein typically measured in rural environments under summertime conditions (e.g. [Lamanna and Goldstein, 1999](#); [Benning and Wahner, 1998](#); [Goldan et al., 1997](#); [Solberg et al., 1996](#); [Montzka et al., 1995](#)).

The atmospheric lifetimes of OH and RO₂ were calculated on the basis of the respective modeled radical fluxes. The calculated lifetime of OH was ≤ 0.5 s throughout the four days considered using the model. The RO_x lifetime was much longer due to the lower reactivity of peroxy radicals. For daytime conditions, it was estimated to be less than 3 minutes, and for nighttime conditions (approximately 19:00 to 07:00 CET) the lifetime was less than 8 minutes for the base case. The RO₂ lifetime is expected to be even longer than this under real nighttime conditions, as HO₂ is removed more quickly than RO₂. HO₂ is the main nighttime sink of RO₂, so that following the drop in HO₂ mixing ratios RO₂ levels will drop much more slowly.

The nighttime chemistry is complicated by the potentially large production of RO_x via the oxidation of NMHCs by the nitrate radical (Reaction 18 in Table 2), and the production of OH from alkene-ozone reactions (Reaction 17 in Table 2). The nitrate radical was not measured during HOPE 2000. However, the production rate of NO₃ radicals can be calculated from the O₃ and NO₂ concentrations. During HOPE 2000, the lifetime of NO₃ radicals with respect to the reaction with NMHC was estimated to range from 25 s to 130 s at night, which is comparable or slightly longer than the lifetime of 20 s to 50 s estimated for the reaction of NO₃ with NO₂. Since the nighttime temperature

Hohenpeissenberg Photochemistry Experiment

Handsides et al.

[Title Page](#)

[Abstract](#)

[Introduction](#)

[Conclusions](#)

[References](#)

[Tables](#)

[Figures](#)

◀

▶

◀

▶

[Back](#)

[Close](#)

[Full Screen / Esc](#)

[Print Version](#)

[Interactive Discussion](#)

© EGU 2002

was about 20°C, N₂O₅ could not build up significantly due to thermal decomposition. Consequently, heterogenous loss of N₂O₅ to aerosol particles was assumed to be a minor loss process for NO₃ compared to the reaction of NO₃ with NMHCs. Thus, the nighttime RO₂ concentration calculated from the NO₃ production rate represents an upper limit. Nighttime RO₂ production rates were calculated to be on the order of 10⁶ molecule cm⁻³ s⁻¹. During the early evening, the ratio between the amount of NO₃ lost due to the reaction with NO₂ and the amount lost due to the reaction with NMHC is highest. This suggests that RO_X production is most likely to be overestimated by the model at this time of day. This is also evident in Fig. 9. The NO₃ radical is quickly photolysed during daytime, so that the effect of RO_X production via NO₃ oxidation of NMHCs was only considered in the model for nighttime conditions.

4.2. OH balance

The measured OH concentrations are compared with the results of the photostationary state calculation for OH in Fig. 7. Considering the 2- σ accuracy of 39% in the OH measurements and the uncertainties in the model, the results agree well with measurements. While the agreement is good for 18, 20 and 21 June, the concentration of OH was overestimated on 19 June. During the late morning on the 19th, the difference between measured and modeled concentrations was relatively high: At 11:00 CET the measured OH concentration was 7.4×10^6 molecule cm⁻³, and was overestimated by about 100% by the calculated concentration of 15.7×10^6 molecule cm⁻³. The ambient NO_x levels measured during the late morning periods (8:00–11:00 CET) of 19 and 20 June showed substantial short term variability, which often exceeded a factor of 2 for consecutive measurements made with a 3 min time resolution. Both NO and NO₂ were measured alternatingly by the same instrument (see Table 1). As a result, the NO and NO₂ mixing ratios for these morning periods are relatively uncertain, possibly by more than a factor of 2 at certain times. Due to the dominant role of the reaction between HO₂ and NO during these periods, the corresponding calculated radical con-

Hohenpeissenberg Photochemistry Experiment

Handsides et al.

[Title Page](#)

[Abstract](#)

[Introduction](#)

[Conclusions](#)

[References](#)

[Tables](#)

[Figures](#)

◀

▶

◀

▶

[Back](#)

[Close](#)

[Full Screen / Esc](#)

[Print Version](#)

[Interactive Discussion](#)

Hohenpeissenberg Photochemistry Experiment

Handsides et al.

[Title Page](#)

[Abstract](#)

[Introduction](#)

[Conclusions](#)

[References](#)

[Tables](#)

[Figures](#)

◀

▶

◀

▶

[Back](#)

[Close](#)

[Full Screen / Esc](#)

[Print Version](#)

[Interactive Discussion](#)

© EGU 2002

centrations are also relatively uncertain. However, this should only affect the variability in the calculated concentrations, and cannot explain the systematic overestimate of the OH concentration by the model. Although the cause of this discrepancy at high NO and NO₂ mixing ratios remains unclear, it is possible that an additional sink for OH was present during the late morning advection episode that is not accounted for in the model. On the other hand, the presence of a large unknown OH sink which was also a RO_X source could lead to an overestimate of the RO_X concentration.

The general shape of the OH diurnal profile, with a maximum in the late morning and lower concentrations in the afternoon, is well reproduced by the photostationary state calculations on all days. The calculated nighttime OH concentrations of up to 5.9×10^5 molecules cm⁻³ were generally slightly higher than the measured concentrations, which were always below the detection limit of 4×10^5 molecules cm⁻³. This is most likely due to the combined effect of a deviation of the HO₂/RO₂ partitioning ratio from 1:1 (as will be discussed in Sect. 4.4), and of NO mixing ratios at the detection limit, which have an uncertainty of a factor of 2.

In order to better understand the relative contributions of the individual sources and sinks to the diurnal profile of the OH concentration, the contributions were calculated using the measurements and are plotted in Fig. 8. The upper panel shows the contributions of the individual source terms to the total production rate; the lower panel shows the contributions of the sink terms. Table 4 gives the average daytime contribution of the source and sink reactions considered in the model, as well as the contribution at 12:00 CET averaged over the four days considered here.

The dominant source of OH radicals turned out to be the recycling of OH via the reaction of HO₂ radicals with NO. This was most pronounced during the late morning episodes of elevated NO_X mixing ratios, when over 50% of the OH radicals were produced by this pathway on average. During periods with relatively low NO mixing ratios below about 100 pptv (e.g. on 18 June and on the afternoons of 20 and 21 June) the primary production of OH via the photolysis of O₃ was comparable to the amount of OH recycled from HO₂. Overall, other relevant reactions, e.g. the reaction between HO₂

**Hohenpeissenberg
Photochemistry
Experiment**

Handisides et al.

[Title Page](#)[Abstract](#)[Introduction](#)[Conclusions](#)[References](#)[Tables](#)[Figures](#)[◀](#)[▶](#)[◀](#)[▶](#)[Back](#)[Close](#)[Full Screen / Esc](#)[Print Version](#)[Interactive Discussion](#)

© EGU 2002

and O₃, alkenes and O₃, and the photolysis of H₂O₂, made only minor contributions to the OH concentration.

The main sink for OH was its reaction with NMHCs. This reaction accounted for an average of 46% of OH loss between 7:00 and 17:00 CET and for 53% loss at 12:00 5 CET. The loss of OH due to the oxidation of CO was nearly equal to the loss to be expected for an assumed 3 ppbv HCHO. The loss of OH due to the oxidation of CH₄ was even less significant, as was the loss due to reactions with H₂, H₂O₂ and HO₂. The reaction of OH with NO₂ was generally only a minor sink, but during the mid-morning advection of polluted air to the measurement site it accounted for up to 25% of the OH 10 loss.

OH concentrations showed a net maximum in the late morning due to the presence of strongly enhanced levels of NO. This tends to shift radicals from RO_X to OH via reactions 11 and 15 in Table 2. In the afternoon hours, however, NO mixing ratios were much lower and the mixing ratios of biogenic hydrocarbons showed a broad maximum. 15 Taken together, these factors caused an increasing shift from OH towards RO_X (see following section).

4.3. RO_X balance

The results for the photostationary state model calculations of RO_X are compared with the measured RO_X mixing ratios in Fig. 9. The agreement between the measured and 20 modeled RO_X mixing ratios was very good for all days except 19 June, considering the uncertainties in both the present simple model approach and the RO_X measurements. Most of the details in the measured RO_X profiles are well reproduced by the model. The dip in the mixing ratio for RO_X at about 8:00 CET is reproduced well on both 19 and 20 June. This dip in the RO_X mixing ratio coincided with a rapid increase in the 25 OH concentration in conjunction with the advection of NO_x enriched boundary layer air from the valley to the measurement site.

The agreement between calculations and measurements was not as good on 19 June for both OH and RO_X, with deviations for RO_X of up to 23 pptv. This discrepancy

was not only observed during the late morning as on other days, but continued into the afternoon hours (Fig. 9). Changes in the composition of the air masses which were not accounted for by the model are probably responsible for this discrepancy. As discussed in Sect. 4.2 above, this suggests that the chemical composition of the system was not adequately determined on 19 June or during the late morning.

In analogy to Fig. 8, individual source and sink strengths for RO_x are shown in Fig. 10. Most daytime sources of RO_x result from the reaction of OH with NMHCs, CO, H_2 , and H_2O_2 . RO_x is also produced as a result of the photolysis of HCHO (Reaction 7). The combined contribution of the oxidation and photolysis of carbonyl compounds turns out to be the second most important source of RO_x , and is equivalent to slightly more than half of the contribution from the oxidation of NMHCs by OH. The relative magnitudes of the source reactions are equal to those of the corresponding OH sinks discussed in the last section.

By far the most dominant sink for RO_x was found to be the reaction of RO_2 radicals with NO. As previously discussed, this was most pronounced during the conversion of HO_2 to OH during the mid to late morning. By comparison, the relative importance of the other sink reactions was almost negligible during these periods. The sink reaction of NO and RO_2 causes a slower build up of RO_x radicals relative to the diurnal increase of OH and radiation and a shift of the maximum RO_x mixing ratio to mid afternoon.

Following the drop in the NO concentration around midday on all days except 19 June, reactions between peroxy radicals and the reaction of RO_x with O_3 become more important, so that eventually more RO_x radicals are lost due to these reactions than due to the loss reaction with NO. The reactions between HO_2 and RO_2 , and the self reaction of HO_2 (Reactions 13 and 14 in Table 2) are the dominant reactions between peroxy radicals. In the base case scenario, HO_2 and RO_2 were assumed to be present in equal amounts, so that the respective turnover rates are similar in magnitude.

Hohenpeissenberg Photochemistry Experiment

Handisides et al.

[Title Page](#)

[Abstract](#)

[Introduction](#)

[Conclusions](#)

[References](#)

[Tables](#)

[Figures](#)

◀

▶

◀

▶

[Back](#)

[Close](#)

[Full Screen / Esc](#)

[Print Version](#)

[Interactive Discussion](#)

[Title Page](#)[Abstract](#)[Introduction](#)[Conclusions](#)[References](#)[Tables](#)[Figures](#)[◀](#)[▶](#)[◀](#)[▶](#)[Back](#)[Close](#)[Full Screen / Esc](#)[Print Version](#)[Interactive Discussion](#)

© EGU 2002

4.4. Testing the model assumptions

The effect of the various assumptions made in the model was also investigated. This was done by running the model for various scenarios with different assumptions about the composition and chemistry of the RO_X radicals. The results for the different scenarios are shown in Fig. 11. Scenario I ignored the production of RO₂ via the nighttime oxidation of alkenes by the NO₃ radical, and fails to produce the significant RO_X levels measured at night. However, as shown by the comparison with measurements in Fig. 11, the nighttime production of RO_X by the NO₃ radical cannot be ignored for the conditions prevailing during HOPE 2000. Although the nighttime NO₃ levels have only been estimated, the results indicate that nighttime oxidation of alkenes via NO₃ oxidation must have been the major cause of the observed nighttime RO_X radicals.

In Scenario II, the assumption was made that, due to the high concentrations of biogenic terpenes, the concentration of RO₂ was twice that of HO₂. Measurements of this ratio during the BERLIOZ campaign by Platt et al. (2002) have shown that this ratio can vary considerably, both on a day-to-day basis and during the course of the same day. The assumption with respect to this ratio was found to have the largest impact on the calculated RO_X mixing ratios in comparison with the other scenarios. This also demonstrates the limitations in the available data base and the need for further more detailed RO_X and HO₂ measurements.

OH concentrations calculated using scenario II are presented in Fig. 12. The results were systematically lower by an average of 30% than the base case scenario and were generally lower than or comparable to the corresponding measured data. Two exceptions occurred during daytime on 19 June, when the calculated OH concentrations exceeded measured concentrations by more than the uncertainty range for the measurements (39%). Nevertheless, Scenario II resulted in an improved agreement between modeled and measured OH concentrations in most cases, with the exception of 21 June.

The effect of a predominance of those RO₂ species whose reactions differ substan-

tially from those of the CH_3O_2 radical was investigated using Scenarios III-V. Scenario III assumed that the reaction of RO_2 with NO (Reaction 10 in the introduction) and the subsequent Reaction 11 only resulted in a 50% nett yield of HO_2 . A reduction in the HO_2 yield can occur for longer chain peroxy radicals due to a higher yield of RONO_2 via the reaction between RO_2 and NO, and for RO radicals which react relatively slowly, or not at all, with O_2 . In Scenario IV, reaction coefficients more typical of longer chain peroxy radicals were used for the RO_2 reactions, instead of the corresponding CH_3O_2 reaction coefficients. Each of these scenarios resulted in an average reduction of the RO_x concentrations by 10-20%. In Scenario V, the yield of RO_x from alkene ozonolysis was assumed to be 50%. The results from this scenario showed that this potential source of RO_x contributed to an increase of less than 5% for daytime RO_x mixing ratios.

The assumption of equal partitioning between HO_2 and RO_2 used in the model is not justified for nighttime conditions since the HO_2 radical is removed much more quickly from the atmosphere than RO_2 , due to the faster reaction of HO_2 with other peroxy radicals. This removes a major sink for RO_2 during the night. By assuming a 1:1 partitioning, the nighttime RO_x mixing ratio may be slightly underestimated, although NO_3 chemistry probably dominates the nighttime budget of RO_x . In comparison, this assumption had a much stronger effect on the calculated nighttime OH concentrations.

The HO_2 reaction with NO was calculated to be the dominant source of night time OH production, compared to the ozonolysis of alkenes. Modeled nighttime OH concentrations using the base case scenario reached levels up to 5.9×10^5 molecules cm^{-3} , whereas measured concentrations were below the detection limit of 4×10^5 molecules cm^{-3} . In contrast, calculated values using the HO_2/RO_2 ratios of scenario II were at or below 4×10^5 molecules cm^{-3} .

Hohenpeissenberg Photochemistry Experiment

Handisides et al.

[Title Page](#)

[Abstract](#)

[Introduction](#)

[Conclusions](#)

[References](#)

[Tables](#)

[Figures](#)

◀

▶

◀

▶

[Back](#)

[Close](#)

[Full Screen / Esc](#)

[Print Version](#)

[Interactive Discussion](#)

5. Conclusions

The present measurements and model results demonstrate the potentially important role of HO_x recycling in determining the temporal profiles of both OH and RO_x at a rural background station such as Hohenpeissenberg. Using a relatively simple photo-stationary state radical balance model constrained by measured data, it was possible to reproduce the main features of the diurnal profiles of both these radicals during the measurement period of 18–21 June 2000 considered here.

RO_x mixing ratios were observed to peak in the early afternoon. This is quite different to the maximum in the OH concentration which occurred during the late morning hours. This can be understood on the basis of the relative contributions of the dominant source and sink terms contributing to the HO_x cycle calculated using the model. It was found that RO_x accumulates over the course of the day as it is produced by NMHC oxidation, with maximum RO_x production occurring at the time of the maximum OH concentration. The presence of elevated NO levels (as observed in the late morning hours) suppresses RO_x levels due to their rapid reaction with NO, which produces NO₂. At the same time, this leads to rapid regeneration of OH and the observed peak concentrations of OH. During the HOPE 2000 campaign, the maximum mixing ratio of NO occurred during late morning and was associated with the transport of polluted air from the boundary layer.

Although the recycling of OH/HO₂ dominates both profiles, the OH concentration is also suppressed during the daylight hours due to its rapid reaction with NMHCs. The biogenic NMHCs, particularly isoprene, were present at quite high mixing ratios during the day, and were the main sink for the OH radical.

Under the conditions experienced during HOPE 2000, biogenic hydrocarbons were a major source of RO₂. Therefore, it seems reasonable to conclude that longer chain RO₂ may have made a significant contribution to the total RO_x mixing ratios. This may have resulted in higher RO₂/HO₂ ratios than used for the base run due to the slower reaction of these long chain RO₂ with other RO₂ and a faster reaction with HO₂. The

Hohenpeissenberg Photochemistry Experiment

Handsides et al.

[Title Page](#)

[Abstract](#)

[Introduction](#)

[Conclusions](#)

[References](#)

[Tables](#)

[Figures](#)

◀

▶

◀

▶

[Back](#)

[Close](#)

[Full Screen / Esc](#)

[Print Version](#)

[Interactive Discussion](#)

© EGU 2002

yield of organic nitrates from the reaction with NO may also have been higher, slowing down the recycling of RO_x to OH. Thus, the conditions encountered during HOPE 2000 may be best approximated by a combination of scenarios II, III and V to describe the RO_x chemistry. However, the combined effects of these scenarios were relatively small and partially compensated one another. Thus, the base case scenario should still describe the situation well.

A previous campaign also conducted in a similar rural and forested environment to HOPE 2000 was the PROPHET campaign. High mixing levels of biogenic hydrocarbons and low NO levels of 40–100 pptv were reported (Tan et al., 2001). The NO levels were comparable to the afternoon mixing ratios during HOPE 2000. The PROPHET calculations using the Regional Atmospheric Chemistry Model (RACM) resulted in OH concentrations which were a factor of 2.7 lower than the measured values. This discrepancy was largest at low NO levels. Although various factors of potential importance were considered by Tan et al. (2001), they could not adequately explain the large difference between modeled and measured OH concentrations.

Oxygenated NMHCs such as HCHO are an important group of trace gases which have a significant effect on the OH balance. The current study assumed the presence of 3 ppbv HCHO as a proxy for oxygenated NMHCs, which resulted in a 20–30% increase in calculated RO_x mixing ratios. While the assumption of 3 ppbv HCHO may be a good average approximation for summertime conditions, real mixing ratios may have varied significantly during the course of the HOPE 2000 campaign. The missing oxygenated NMHCs, especially HCHO, is a major deficit of HOPE 2000, and these compounds need to be taken into greater consideration in future campaigns.

Although a number of recent studies, including HOPE 2000, have attempted to achieve closure of the OH and RO_x budgets, the results show that this aim cannot currently be considered to have been achieved. In addition to the requirement of including additional components in the measurements, e.g. of aldehydes and ketones, the current study underlines the importance of constraining the HO_2/RO_2 partition ratio by RO_x radical measurements in future studies.

Hohenpeissenberg Photochemistry Experiment

Handisides et al.

[Title Page](#)

[Abstract](#)

[Introduction](#)

[Conclusions](#)

[References](#)

[Tables](#)

[Figures](#)

◀

▶

◀

▶

[Back](#)

[Close](#)

[Full Screen / Esc](#)

[Print Version](#)

[Interactive Discussion](#)

Acknowledgements. The authors wish to thank T. Elste, K. Michl, G. Stange, R. T. Wilhelm and the staff of the Meteorological Observatory Hohenpeissenberg for their assistance during HOPE, and U. Schmidt of the Institute for Meteorology and Geophysics, Frankfurt am Main, for his support. The Peroxy Radical Chemical Amplifier was financed by the Hessische Landesamt für Umwelt und Geologie.

References

- Abram, J., Creasey, D. J., Heard, D. E., Lee, J. D., and Pilling, M. J.: Hydroxyl radical and ozone measurements in England during the solar eclipse of 11 August 1999, *Geophys. Res. Lett.*, 27, 3437–3440, 2000. [2510](#)
- Atkinson, R.: Gas-phase Tropospheric Chemistry of Organic Compounds, *J. Phys. Chem. Ref. Data*, Monograph 2, 1–216, 1994. [2539](#), [2540](#)
- Atkinson, R.: Gas-phase tropospheric chemistry of Volatile Organic Compounds: 1. Alkanes and Alkenes, *J. Phys. Chem. Ref. Data*, 26, 215–290, 1997. [2518](#), [2521](#), [2538](#), [2539](#), [2540](#), [2541](#)
- Atkinson, R.: Atmospheric chemistry of VOCs and NO_x, *Atm. Environ.*, 34, 2063–2101, 2000. [2509](#)
- Atkinson, R. and Aschmann, S. M.: OH radical reaction rate constants for polycyclic alkanes: effects of ring strain and consequences for estimation methods, *Int. J. Chem. Kinet.*, 22, 983–989, 1992. [2541](#)
- Atkinson, R., Baulch, D. L., Cox, R. A., Hampson, Jr., R. F., Kerr, J. A., Rossi, M. J., Troe, J.: Evaluated kinetic and photochemical data for atmospheric chemistry, organic species: Supplement VII, *J. Phys. Chem. Ref. Data*, 28, 2, 191–393, 1999. [2539](#)
- Atkinson, R., Baulch, D. L., Cox, R. A., Crowley, J. N., Hampson, Jr., R. F., Kerr, J. A., Rossi, M. J., and Troe, J.: Summary of Evaluated Kinetic and Photochemical Data for Atmospheric Chemistry: IUPAC Subcommittee on Gas Kinetic Data Evaluation for Atmospheric Chemistry, Web Version, <http://www.iupac-kinetic.ch.cam.ac.uk/>, 2001. [2537](#)
- Benning, L. and Wahner, A.: Measurements of atmospheric formaldehyde (HCHO) and acetaldehyde (CH₃CHO) during POPCORN 1994 using 2.4-DNPH coated silica cartridges, *J. Atmos. Chem.*, 31, 105–117, 1998. [2522](#)
- Berresheim, H., Elste, T., Plass-Dülmer, C., Eisele, F. L., and Tanner, D.: Chemical ionization

Hohenpeissenberg Photochemistry Experiment

Handsides et al.

[Title Page](#)

[Abstract](#)

[Introduction](#)

[Conclusions](#)

[References](#)

[Tables](#)

[Figures](#)

◀

▶

◀

▶

[Back](#)

[Close](#)

[Full Screen / Esc](#)

[Print Version](#)

[Interactive Discussion](#)

© EGU 2002

Hohenpeissenberg Photochemistry Experiment

Handisides et al.

[Title Page](#)

[Abstract](#)

[Introduction](#)

[Conclusions](#)

[References](#)

[Tables](#)

[Figures](#)

◀

▶

◀

▶

[Back](#)

[Close](#)

[Full Screen / Esc](#)

[Print Version](#)

[Interactive Discussion](#)

© EGU 2002

mass spectrometer for long-term measurements of atmospheric OH and H₂SO₄, Int. J. Mass Spectrom., 202, 91–103, 2000. [2512, 2513](#)

Cantrell, C. A., Stedman, D. H., and Wendel, G. J.: Measurement of atmospheric peroxy radicals by chemical amplification, Ana. Chem., 56, 1496–1502, 1984. [2513](#)

Cantrell, C. A., Shetter, R. E., Gilpin, T. M., and Calvert, J. G.: Peroxy radicals measured during Mauna Loa Observatory Photochemistry Experiment 2 - The data and first analysis, J. Geophys. Res., 101, 14,643–14,652, 1996. [2513](#)

Cantrell, C. A., Shetter, R. E., Calvert, J. G., Eisele, F. L., Williams, E., Baumann, K., Brune, W. H., Stevens, P. S., and Mather, J. H.: Peroxy radicals from photostationary state deviations and steady state calculations during the Tropospheric OH Photochemistry Experiment at Idaho Hill, Colorado, 1993, J. Geophys. Res., 102, 6369–6378, 1997a. [2510](#)

Cantrell, C. A., Zimmer, A., and Tyndall, G. S.: Absorption cross sections for water vapour from 183 to 193 nm, Geophys. Res. Lett., 24, 2195–2198, 1997b. [2513](#)

Carroll, M. A., Bertman, S. B., and Shepson, P. B.: Overview of the Program for Research on Oxidants: PHotochemistry, Emissions, and Transport (PROPHET) summer 1998 measurements intensive, J. Geophys. Res., 106, 24,275–24,288, 2001. [2511](#)

Carlsaw, N., Creasey, D. J., Heard, D. E., Lewis, A. C., McQuaid, J. B., Pilling, M. J., Monks, P. S., Bandy, B. J., and Penkett, S. A.: Modeling OH, HO₂, and RO₂ radicals in the marine boundary layer – 1. model construction and comparison with field measurements, J. Geophys. Res., 104, 30 241–30 255, 1999. [2510, 2511](#)

Carlsaw, N., Creasey, D. J., Harrison, D., Heard, D. E., Hunter, M. C., Jacobs, P. J., Jenkin, M. E., Lee, J. D., Lewis, A. C., Saunders, M. J. P. S. M., and Seakins, P. W.: OH and HO₂ radical chemistry in a forested region of north-western Greece, Atm. Environ., 35, 4725–4737, 2001. [2510](#)

Carlsaw, N., Creasey, D. J., Heard, D. E., Jacobs, P. J., Lee, J. D., Lewis, A. C., McQuaid, J. B., Pilling, M. J., Bagutte, S., Penkett, S. A., Monks, P. S., and Salisbury, G.: Eastern Atlantic Spring Experiment 1997 (EASE97) 2. Comparisons of model concentrations of OH, HO₂, and RO₂ with measurements, J. Geophys. Res., 107, 10.1029/2001JD001568, 2002. [2509, 2510, 2511, 2513, 2521](#)

Corchnoy, S. B. and Atkinson, R.: Kinetics of the gas-phase reactions of OH and NO₃ radicals with 2-carene, 1,8-cineole, p-cymene, and terpinolene, Environ. Sci. Technol., 24, 1497–1502, 1990. [2541](#)

Creasey, D. J., Heard, D. E., and Lee, J. D.: Eastern Atlantic Spring Experiment 1997 (EASE97)

Hohenpeissenberg Photochemistry Experiment

Handisides et al.

1. Measurements of OH and HO₂ concentrations at Mace Head, Ireland, J. Geophys. Res., 107, 10.1029/2001JD000892, 2002. [2510](#)
- George, L. A., Hard, T. M., and O'Brien, R. J.: Measurement of free radicals OH and HO₂ in Los Angeles smog, J. Geophys. Res., 104, 11 643–11 656, 1999. [2510](#), [2511](#)
- Goldan, P. D., Kuster, W. C., Fehsenfeld, F. C., and Montzka, S. A.: Hydrocarbon measurements in the southeastern United States: The Rural Oxidants in the Southern Environment (ROSE) Program 1990, J. Geophys. Res., 100, 25 945–25 963, 1995. [2515](#)
- Goldan, P. D., Kuster, W. C., and Fehsenfeld, F. C.: Nonmethane hydrocarbon measurements during the Tropospheric OH Photochemistry Experiment, J. Geophys. Res., 102, 6315–6324, 1997. [2522](#)
- Guenther, A. B., Zimmerman, P., Harley, P., Monson, R., and Fall, R.: Isoprene and monoterpene emission rate variability: Model evaluation and sensitivity analysis, J. Geophys. Res., 98, 12 609–12 617, 1993. [2519](#)
- 15 Handisides, G. M.: The Influence of Peroxy Radicals on Ozone Production, Dissertation, Johann-Wolfgang-Goethe University, Frankfurt am Main, <http://dbib.uni-frankfurt.de/diss-cgi/show/meta?signatur=00000231>, 2001. [2513](#)
- Hastie, D. R., Weissenmayer, M., Burrows, J. P., and Harris, G. W.: Calibrated chemical amplifier for atmospheric RO_x measurements, Anal. Chem., 63, 2048–2057, 1991. [2513](#), [2514](#)
- 20 Helmig, D., Greenberg, J., Guenther, A., Zimmerman, P., and Geron, C.: Volatile organic compounds and isoprene oxidation products at a temperate deciduous forest site, J. Geophys. Res., 103, 22 397–22 414, 1998. [2515](#)
- Kwok, E. S. C. and Atkinson, R.: Estimation of Hydroxyl Radical Reaction Rate Constants for Gas-Phase Organic Compounds using a Structure-Reactivity Relationship: an Update, Atm. Environ., 29, 1685–1695, 1995. [2540](#), [2541](#)
- 25 Lamanna, M. S. and Goldstein, A. H.: In situ measurements of C₂-C₁₀ volatile organic compounds above a Sierra Nevada ponderosa pine plantation, J. Geophys. Res., 104, 21 247–21 262, 1999. [2522](#)
- Mather, J. H., Stevens, P. S., and Brune, W. H., OH and HO₂ measurements using laser-induced fluorescence, J. Geophys. Res., 102, 6427–6436, 1997. [2510](#)
- 30 McKeen, S. A., Mount, G., Eisele, F., Williams, E., Harder, J., Goldan, P., Kuster, W., Liu, S. C., Baumann, K., Tanner, D., Fried, A., Sewell, S., Cantrell, C., and Shetter, R.: Photochemical modelling of hydroxyl and its relationship to other species during the Tropospheric OH Photochemistry Experiment, J. Geophys. Res., 102, 6467–6493, 1997. [2510](#)

Title Page	
Abstract	Introduction
Conclusions	References
Tables	Figures
◀	▶
◀	▶
Back	Close
Full Screen / Esc	
Print Version	
Interactive Discussion	

- Mihelcic, D., Volz-Thomas, A., Pätz, H. W., and Kley, D.: Numerical analysis of ESR spectra from atmospheric samples, *J. Atmos. Chem.*, 11, 271–297, 1990. [2513](#)
- Mihelcic, D., Klemp, D., Musgen, P., Patz, H., and Volz-Thomas, A.: Simultaneous measurements of peroxy and nitrate radicals at Schauinsland, *J. Atmos. Chem.*, 16, 313–335, 1993. [2521](#)
- Mihelcic, D., Konrad, S., Pätz, H.-W., Schmitz, T., Volz-Thomas, A., Holland, F., Hofzumahaus, A., Bächmann, H.-J. K., Geyer, A., and Perner, D.: Comparison of measurements of OH, HO₂ and RO₂ radicals during the BERLIOZ campaign., presented at 8th IAMAS Scientific Assembly, Innsbruck, Austria, 2001. [2521](#)
- Mihele, C. M. and Hastie, D. R.: The sensitivity of the radical amplifier to ambient water vapour, *Geophys. Res. Lett.*, 25, 1911–1913, 1998. [2514](#)
- Mihele, C. M. and Hastie, D. R.: Optimized operation and calibration procedures for radical amplifier-type detectors, *J. Atmos. Ocean Technol.*, 17, 788–794, 2000. [2514](#)
- Mihele, C. M., Mozurkewich, M., and Hastie, D. R.: Radical loss in a chain reaction of CO and NO in the presence of water: Implications for the radical amplifier and atmospheric chemistry, 31, 145–152, 1999. [2514](#)
- Monks, P. S., Carpenter, L. J., Penkett, S. A., and Ayers, G. P.: Night-time peroxy radical chemistry in the remote boundary layer over the Southern Ocean, *Geophys. Res. Lett.*, 23, 535–538, 1996. [2513](#)
- Montzka, S. A., Trainer, M., Angevine, W. M., and Fehsenfeld, F. C.: Measurements of 3-methyl furan, methyl vinyl ketone, and methacrolein at a rural forested site in the southeastern United States, *J. Geophys. Res.*, 100, 11 393–11 401, 1995. [2522](#)
- Mount, G. H., Brault, J. W., Johnston, P. V., Marovich, E., Jakoubek, R. O., Volpe, C. J., Harder, J., and Olson, J.: Measurement of tropospheric OH by long-path laser absorption at Fritz Peak Observatory, Colorado, during the OH Photochemistry Experiment, fall 1993, *J. Geophys. Res.*, 102, 6393–6413, 1997. [2510](#)
- Novelli, P. C., Lang, P. M., Masarie, K. A., Hurst, D. F., Meyers, R., and Elkins, J. W.: Molecular hydrogen in the troposphere: Global distribution and budget, *J. Geophys. Res.*, 104, 30 427–30 444, 1999. [2522](#)
- Plass-Dülmer, C., Michl, K., Ruf, R., and Berresheim, H.: C₂-C₈ hydrocarbon measurement and quality control procedures at the Global Atmosphere Watch Observatory Hohenpeissenberg, *J. Chromatogr. A*, 953, 175–197, 2002. [2515](#), [2516](#)
- Platt, U., Aliche, B., Dubois, R., Geyer, A., Hofzumahaus, A., Holland, F., Martinez, M., Mihelcic,

Hohenpeissenberg Photochemistry Experiment

Handsides et al.

[Title Page](#)

[Abstract](#)

[Introduction](#)

[Conclusions](#)

[References](#)

[Tables](#)

[Figures](#)

◀

▶

◀

▶

[Back](#)

[Close](#)

[Full Screen / Esc](#)

[Print Version](#)

[Interactive Discussion](#)

- D., Klüpfel, T., Lohrmann, B., Pätz, W., Perner, D., Rohrer, F., Schäfer, J., and Stutz, J.: Free radicals and fast photochemistry during BERLIOZ, *J. Atmos. Chem.*, 42, 359–394, 2002. [2510](#), [2513](#), [2527](#)
- 5 Poppe, D., Zimmermann, J., Bauer, R., Brauers, T., Brüning, D., Callies, J., Dorn, H.-P., Hofzumahaus, A., Johnen, F.-J., Khedim, A., Koch, H., Koppmann, R., London, H., Müller, K., Neuroth, R., Plass-Dülmer, C., Platt, U., an E.-P. Röth, F. R., Rudolph, J., Schmidt, U., Wallasch, M., and Ehhalt, D. H.: Comparison of measured OH concentrations with model calculations, *J. Geophys. Res.*, 99, 16 633–16 642, 1994. [2509](#)
- 10 Reichert, L.: Untersuchung des Wassereffektes eines Peroxyradikal-Detektors, Diplomarbeit, Institut für Umweltphysik, Universität Bremen, Bremen, 2000. [2514](#)
- Riemer, D., Milne, P. J., Farmer, C. T., and Zika, R.: Determination of terpene and related compounds in semi-urban air by GC-MSD, *Chemosphere*, 28, 837–850, 1994. [2515](#)
- 15 Ruggaber, A., Dlugi, R., and Nakajima, T.: Modelling of radiation quantities and photolysis frequencies in the troposphere, *J. Atmos. Chem.*, 27, 171–210, 1994. [2521](#)
- Schultz, M., Heitlinger, M., Mihelcic, D., and Volz-Thomas, A.: Calibration source for peroxy radicals with built-in actinometry using H_2O and O_2 photolysis at 185 nm, *J. Geophys. Res.*, 100, 18 811–18 816, 1995. [2514](#)
- 20 Schwander, H., Koepke, P., Ruggaber, A., Nakajima, T., Kaifel, A., and Oppenrieder, A.: STARSci 2.1: System for Transfer of Atmospheric Radiation, <http://www.meteo.physik.uni-muenchen.de/strahlung/uvrad/Star/STARinfo.htm>, 2001. [2521](#)
- Semadeni, M., Stocker, D. W., and Kerr, J. A.: The temperature dependence of the OH radical reactions with some aromatic compounds under simulated tropospheric conditions, *Int. J. Chem. Kinet.*, 27, 287–304, 1995. [2539](#), [2540](#)
- 25 Solberg, S., Dye, C., Schmidbauer, N., Herzog, A., and Gehrig, R.: Carbonyls and nonmethane hydrocarbons at rural European sites from the Mediterranean to the Arctic, *J. Atmos. Chem.*, 25, 33–66, 1996. [2522](#)
- Tan, D., Faloona, I., Simpas, J., Brune, W., Shepson, P., Couch, T., Summer, A., Carroll, M., Thornberry, T., Apel, E., Riemer, D., and Stockwell, W.: HO_x budgets in a deciduous forest: 30 Results from the PROPHET summer 1998 campaign, *J. Geophys. Res.*, 106, 24 407–24 427, 2001. [2510](#), [2511](#), [2530](#)
- Tanner, D. J., Jefferson, A., and Eisele, F. L.: Selected ion chemical ionization mass spectrometric measurement of OH, *J. Geophys. Res.*, D102, 6415–6425, 1997. [2510](#), [2513](#)
- Umweltbundesamt: Jahresbericht 2000 des Messnetzes, Texte 77/01, Berlin, 2001. [2522](#)

Hohenpeissenberg Photochemistry Experiment

Handsides et al.

[Title Page](#)

[Abstract](#)

[Introduction](#)

[Conclusions](#)

[References](#)

[Tables](#)

[Figures](#)

◀

▶

◀

▶

[Back](#)

[Close](#)

[Full Screen / Esc](#)

[Print Version](#)

[Interactive Discussion](#)

Table 1. Summary of instrumentation used during HOPE, in June and July, 2000

Component	Instrument	Measurement method	Signal Integration Period	Accuracy ^a
TRACE GASES				
OH	DWD-CIMS	Chemical ionisation mass spectrometry	5 min	see text
RO _x	IMG-CA	Chemical amplification	10 min	see text
Ozone	Thermo Instr./Dasibi	UV absorption	1 min	4%, 0.5 ppbv
NO	EcoPhysics	Chemoluminescence Detector (CLD)	3 min	5%, 15 pptv
NO ₂	EcoPhysics	CLD with photolytic converter	3 min	6%, 30 pptv
NO _y	EcoPhysics	CLD with gold converter	4 min	9%, 50 pptv
SO ₂	Thermo Instruments	UV fluorescence	1 min.	5%, 50 pptv
H ₂ O ₂ , ROOH	AeroLaser/Custom built	Enzyme Catalysed Fluorescence	1 min	9%, 100 pptv
CO	Thermo Instruments	IR absorption with gas filter correlation	20 min	5%, 5 ppbv
C ₂ -C ₈ HC	Varian/Custom built	GC/FID	15 min ^b	see text
C ₅ -C ₁₃	Varian/Custom built	GC/MS/FID	20 min ^c	see text
RADIATION				
Global radiation	Kipp & Zonen CM11	Moll thermopile	1 min	3%
J _{O1D}	MetCon, Glashütten	filter radiometer	1 min	25%
J _{NO₂}		filter radiometer	1 min	15%

^a = For each measurement the accuracy is determined by the larger of the two values.

^b = Sample frequency: every 75 min - 6 h.

^c = Sample frequency: every 60 min - 6 h.

Hohenpeissenberg Photochemistry Experiment

Handisides et al.

[Title Page](#)

[Abstract](#)

[Introduction](#)

[Conclusions](#)

[References](#)

[Tables](#)

[Figures](#)

◀

▶

◀

▶

[Back](#)

[Close](#)

[Full Screen / Esc](#)

[Print Version](#)

[Interactive Discussion](#)

Hohenpeissenberg Photochemistry Experiment

Handisides et al.

Table 2. Reactions and rate coefficients used in the photostationary state calculations of the radical concentrations. The role played by the relevant reaction in the respective radical cycle is denoted by P for Production and L for Loss. All rate coefficients have been calculated for a relevant average temperature of 293 K using the temperature dependent rate equations from Atkinson et al. (2001) (where available; otherwise k(298) was used). Rates for termolecular reactions were calculated for P = 908 hPa

No.	Reaction	Role in cycle for			k(293K)
		OH	HO ₂	RO ₂	cm ³ molecule ⁻¹ s ⁻¹
PHOTOLYSIS REACTIONS					
1.	O ₃ + hν $\xrightarrow{H_2O}$ 2OH + O ₂	P			measured ^a
2.	H ₂ O ₂ + hν → 2OH	P			j _{H₂O₂} , STAR Model
3.	HCHO + hν $\xrightarrow{O_2}$ 2HO ₂ + CO	P			j _{HCHO} , STAR Model
OH REACTIONS					
4.	OH + RH → R + H ₂ O $\xrightarrow{O_2}$ RO ₂ + H ₂ O	L	P	P	various ^b
5.	OH + HCHO → HCO + H ₂ O $\xrightarrow{O_2}$ HO ₂ + CO + H ₂ O	L	P		9.2×10 ⁻¹²
6.	OH + CO → H + CO ₂ $\xrightarrow{O_2}$ HO ₂ + CO ₂	L	P		2.0×10 ⁻¹³ ^c
7.	OH + NO ₂ \xrightarrow{M} HNO ₃	L			1.5×10 ⁻¹¹
8.	OH + H ₂ → H + H ₂ O $\xrightarrow{O_2}$ HO ₂ + H ₂ O	L	P		6.7×10 ⁻¹⁵
9.	OH + H ₂ O ₂ → HO ₂ + H ₂ O	L	P		1.7×10 ⁻¹²
10.	OH + HO ₂ → H ₂ O + O ₂	L	L		1.1×10 ⁻¹⁰
HO₂ REACTIONS					
11.	HO ₂ + NO → OH + NO ₂	P	L		8.8×10 ⁻¹²
12.	HO ₂ + O ₃ → OH + 2O ₂	P	L		2.0×10 ⁻¹⁵
13.	HO ₂ + HO ₂ → H ₂ O ₂ + O ₂	L			5.0×10 ⁻¹²
14.	HO ₂ + RO ₂ → ROOH + O ₂	L	L		1.6×10 ⁻¹¹ ^d
14a.	HO ₂ + CH ₃ O ₂ → CH ₃ OOH + O ₂	L	L		5.2×10 ⁻¹²

Title Page	
Abstract	Introduction
Conclusions	References
Tables	Figures
Full Screen / Esc	
Print Version	
Interactive Discussion	

**Hohenpeissenberg
Photochemistry
Experiment**

Handisides et al.

Table 2. (Continued)

No.	Reaction	Role in cycle for OH HO ₂ RO ₂	k(293K) cm ³ molecule ⁻¹ s ⁻¹
RO₂ REACTIONS			
15a.	RO ₂ + NO → RO + NO ₂	L	9.2×10 ⁻¹² ^e
15a'.	CH ₃ O ₂ + NO → CH ₃ O + NO ₂	L	7.5×10 ⁻¹²
15b.	RO ₂ + NO → RONO ₂	L	
16.	RO ₂ + RO ₂ → ROOR	L	
16a.	CH ₃ O ₂ + CH ₃ O ₂ → CH ₃ OOCH ₃	L	3.7×10 ⁻¹³
ALKENE REACTIONS			
17.	O ₃ + Alkene → RO ₂ + products	P	various
18.	NO ₃ + Alkene → RO ₂ + products	P	various

^a = Primary production of OH calculated from measured values; denoted P(OH).

^b = See Table 3.

^c = For P = 908hPa.

^d = For R \geq C₂; recommended value for R \geq C₃ from Atkinson (1997) was used in Scenario IV; the C₂ reaction rate was not considered.

^e = For R \geq C₂; recommended value from Atkinson (1997) was used in Scenario IV.

[Title Page](#)

[Abstract](#)

[Introduction](#)

[Conclusions](#)

[References](#)

[Tables](#)

[Figures](#)

◀

▶

◀

▶

[Back](#)

[Close](#)

[Full Screen / Esc](#)

[Print Version](#)

[Interactive Discussion](#)

Table 3. Daytime average hydrocarbon mixing ratios, measurement accuracies, and OH reaction rate constants used in the steady state model calculations

Substance Name	Average Mixing Ratio 07:00-17:00 CET	Accuracy pptv	$k_{OH}(293K^a, 908\text{hPa})$	Ref.
methane	1.842 ppmv ^b		6.4×10^{-15}	Atkinson et al. (1999)
ethyne	202.1	31.5	7.8×10^{-13}	Atkinson (1994)
ethene	162.0	11.3	8.99×10^{-12}	Atkinson et al. (1999)
ethane	931.1	52.7	2.36×10^{-13}	Atkinson et al. (1999)
propyne	5.0	2.5	5.9×10^{-12} *	Atkinson (1994)
propene	58.9	7.1	3.0×10^{-11}	Atkinson et al. (1999)
propane	193.0	11.2	1.07×10^{-12}	Atkinson et al. (1999)
1,3-butadiene	24.6	3.2	6.83×10^{-11}	Atkinson (1997)
trans-2-butene	8.3	7.5	6.60×10^{-11}	Atkinson (1997)
1-butene	2.8	4.2	3.22×10^{-11}	Atkinson (1997)
2-methylpropene	23.3	22.0	5.28×10^{-11}	Atkinson (1997)
cis-2-butene	5.2	5.0	5.79×10^{-11}	Atkinson (1997)
2-methylpropane	50.3	3.2	2.15×10^{-12}	Atkinson (1997)
isoprene	308.8	67.2	1.03×10^{-10}	Atkinson (1997)
n-butane	86.0	5.0	2.34×10^{-12}	Atkinson et al. (1999)
cyclopentane	3.9	0.8	4.92×10^{-12}	Atkinson (1997)
trans-2-pentene	0.8	1.6	6.7×10^{-11} *	Atkinson (1997)
1-pentene	6.2	3.0	3.14×10^{-11} *	Atkinson (1997)
cis-2-pentene	0.7	1.7	6.50×10^{-11} *	Atkinson (1997)
2-methylbutane	188.9	12.0	3.7×10^{-12} *	Atkinson (1997)
n-pentane	67.5	5.1	3.91×10^{-12}	Atkinson (1997)
benzene	69.0	6.0	1.17×10^{-12}	Semadeni et al. (1995)

Hohenpeissenberg Photochemistry Experiment

Handisides et al.

Title Page

Abstract

Introduction

Conclusions

References

Tables

Figures

◀

▶

◀

▶

Back

Close

Full Screen / Esc

Print Version

Interactive Discussion

© EGU 2002

Table 3. (Continued)

Substance Name	Average Mixing Ratio 07:00-17:00 CET	Accuracy pptv	$k_{OH}(293K^a, 908\text{hPa})$ cm ³ molecule ⁻¹ s ⁻¹	Ref.
methylcyclopentane	11.8	2.4	$6.8 \times 10^{-12}^*$	Kwok and Atkinson (1995)
cyclohexane	13.3	2.1	7.10×10^{-12}	Atkinson (1997)
1-hexene	3.4	1.2	$3.70 \times 10^{-11}^*$	Atkinson (1997)
n-hexane	15.3	1.4	5.40×10^{-12}	Atkinson (1997)
2-methylpentane	37.3	2.8	$5.30 \times 10^{-12}^*$	Atkinson (1997)
3-methylpentane	23.5	1.9	$5.40 \times 10^{-12}^*$	Atkinson (1997)
2,3-dimethylbutane	4.8	1.7	5.75×10^{-12}	Atkinson (1997)
toluene	106.6	7.1	6.4×10^{-12}	Semadeni et al. (1995)
methylcyclohexane	4.1	0.8	$1.00 \times 10^{-11}^*$	Atkinson (1997)
2-methylhexane	9.3	1.4	$5.10 \times 10^{-12}^*$	Kwok and Atkinson (1995)
2,3-dimethylpentane	4.2	1.6	$6.10 \times 10^{-12}^*$	Kwok and Atkinson (1995)
n-heptane	15.7	1.4	6.98×10^{-12}	Atkinson (1997)
ethylbenzene	30.4	1.8	$7.10 \times 10^{-12}^*$	Atkinson (1994)
m,p-xylene	68.8	8.0	$1.90 \times 10^{-11}^*$	Atkinson (1994)
o-xylene	29.9	2.1	$1.37 \times 10^{-11}^*$	Atkinson (1994)
n-octane	5.0	0.9	8.60×10^{-12}	Atkinson (1997)
3-methylheptane	3.9	0.7	$8.56 \times 10^{-12}^*$	Kwok and Atkinson (1995)
4-methylheptane	5.5	1.0	$8.56 \times 10^{-12}^*$	Kwok and Atkinson (1995)
n-propylbenzene	2.6	1.0	$5.70 \times 10^{-12}^*$	Atkinson (1994)
1,3,5-trimethylbenzene	2.1	0.4	$5.75 \times 10^{-11}^*$	Atkinson (1994)
1,2,4-trimethylbenzene	10.4	1.9	$3.75 \times 10^{-11}^*$	Atkinson (1994)
m-ethyltoluene	6.9	2.1	$1.71 \times 10^{-11}^*$	Atkinson (1994)
p-ethyltoluene	3.3	1.0	$1.14 \times 10^{-11}^*$	Atkinson (1994)

Hohenpeissenberg Photochemistry Experiment

Handisides et al.

Title Page

Abstract

Introduction

Conclusions

References

Tables

Figures

◀

▶

◀

▶

Back

Close

Full Screen / Esc

Print Version

Interactive Discussion

Table 3. (Continued)

Substance Name	Average Mixing Ratio	Accuracy 07:00-17:00 CET	$k_{OH}(293K^a, 908\text{hPa})$	Ref.
	pptv		pptv	
			$\text{cm}^3 \text{molecule}^{-1} \text{s}^{-1}$	
n-nonane	9.6	2.9	9.91×10^{-12}	Atkinson (1997)
i-butylbenzene	0.6	0.6	$8.17 \times 10^{-12}^*$	Kwok and Atkinson (1995)
sec-butylbenzene	2.7	1.1	$8.17 \times 10^{-12}^*$	Kwok and Atkinson (1995)
p-cymene	11.5	3.5	1.51×10^{-11}	Crochnoy and Atkinson (1990)
1-methyl-3-propylbenzene	1.4	0.4	$1.47 \times 10^{-11}^*$	Kwok and Atkinson (1995)
α -pinene	131.3	39.5	5.51×10^{-11}	Atkinson (1997)
β -pinene	62.0	19.2	8.05×10^{-11}	Atkinson (1997)
camphene	22.7	7.4	5.3×10^{-11}	Atkinson (1997)
sabinene	59.2	35.0	1.17×10^{-10}	Atkinson (1997)
myrcene	15.9	5.7	2.15×10^{-10}	Atkinson (1997)
3-carene	38.3	14.0	8.8×10^{-11}	Atkinson (1997)
α -terpinene ^c	2.7	2.7	3.63×10^{-10}	Atkinson (1997)
terpinolene	2.9	1.7	2.25×10^{-10}	Atkinson (1997)
γ -terpinene	5.4	2.7	1.77×10^{-10}	Atkinson (1997)
limonene	23.9	7.5	1.71×10^{-10}	Atkinson (1997)
tricyclene	10.0	3.4	$2.86 \times 10^{-12}^*$	Atkinson and Aschmann (1992)
1,8-cineol	29.2	14.5	$1.11 \times 10^{-11}^*$	Crochnoy and Atkinson (1990)
n-undecane	6.1	2.4	$1.29 \times 10^{-11}^*$	Atkinson (1997)
n-dodecane	2.3	0.7	$1.39 \times 10^{-11}^*$	Atkinson (1997)
n-tridecane	1.3	0.6	$1.60 \times 10^{-11}^*$	Atkinson (1997)

^a = A star denotes a rate coefficient for 298K.^b = Average value for June 2002 measured at Schauinsland, see text.^c = Due to its high inaccuracy, α -terpinene was excluded from the data set for the model calculations, see description of the NMHC system for discussion.

Hohenpeissenberg Photochemistry Experiment

Handisides et al.

Title Page

Abstract

Introduction

Conclusions

References

Tables

Figures

◀

▶

◀

▶

Back

Close

Full Screen / Esc

Print Version

Interactive Discussion

Table 4. Average contributions of individual source and sink reactions to the OH balance for the period 18–21 June, 2000

	Daytime Average 7:00-17:00 CET $10^6 \text{ molec. cm}^{-3} \text{ s}^{-1}$	Midday Average 12:00 CET $10^6 \text{ molec. cm}^{-3} \text{ s}^{-1}$
SOURCES		
$\text{HO}_2 + \text{NO}$	13.2	10.6
P(OH)	4.6	7.8
$\text{HO}_2 + \text{O}_3$	0.95	1.3
P(H_2O_2)	0.5	0.7
$\text{O}_3 + \text{Alkenes}$	1.1	1.1
Total Sources	20.2	21.4
SINKS		
NMHC	-7.4	-10.5
CO	-2.4	-2.9
CH_4 (1.842 ppmv)	-1.0	-1.2
HCHO (3 ppbv)	-2.6	-3.2
$\text{H}_2 + \text{H}_2\text{O}_2 + \text{HO}_2$	-0.8	-1.1
NO_2	-2.1	-1.2
Total Sinks	-16.2	-20.1

Hohenpeissenberg Photochemistry Experiment

Handisides et al.

[Title Page](#)

[Abstract](#)

[Introduction](#)

[Conclusions](#)

[References](#)

[Tables](#)

[Figures](#)

◀

▶

◀

▶

[Back](#)

[Close](#)

[Full Screen / Esc](#)

[Print Version](#)

[Interactive Discussion](#)

**Hohenpeissenberg
Photochemistry
Experiment**

Handisides et al.

Table 5. The average contribution of each individual source and sink to the RO_x concentration

	Daytime Average 7:00-17:00	Midday Average
	$10^6 \text{ molec. cm}^{-3} \text{ s}^{-1}$	$10^6 \text{ molec. cm}^{-3} \text{ s}^{-1}$
SOURCES		
NMHC	7.4	10.5
CO	2.4	2.9
CH ₄ (1.842 ppmv)	1.0	1.2
HCHO (3 ppbv)	5.2	6.5
H ₂ +H ₂ O ₂	0.6	0.8
Total Sources	16.5	22.0
SINKS		
HO ₂ +NO	-13.2	-10.6
HO ₂ +RO ₂	-1.8	-2.3
HO ₂ +HO ₂	-1.6	-2.1
HO ₂ +O ₃	-0.9	-1.3
RO ₂ +RO ₂	-0.1	-0.2
HO ₂ +OH	-0.2	-0.3
Total Sinks	-17.8	-16.7

[Title Page](#)

[Abstract](#)

[Introduction](#)

[Conclusions](#)

[References](#)

[Tables](#)

[Figures](#)

◀

▶

◀

▶

[Back](#)

[Close](#)

[Full Screen / Esc](#)

[Print Version](#)

[Interactive Discussion](#)

**Hohenpeissenberg
Photochemistry
Experiment**

Handisides et al.

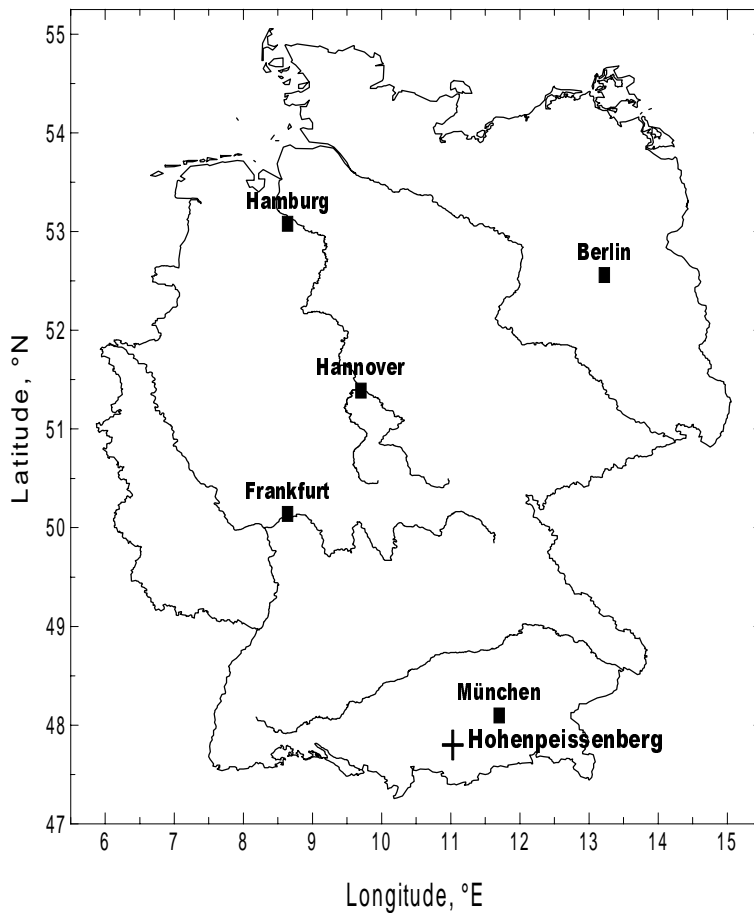


Fig. 1. Map of Germany showing the location of the Meteorological Observatory Hohenpeissenberg (975 m a.s.l.) in southern Bavaria.

[Print Version](#)[Interactive Discussion](#)

© EGU 2002

Hohenpeissenberg Photochemistry Experiment

Handisides et al.

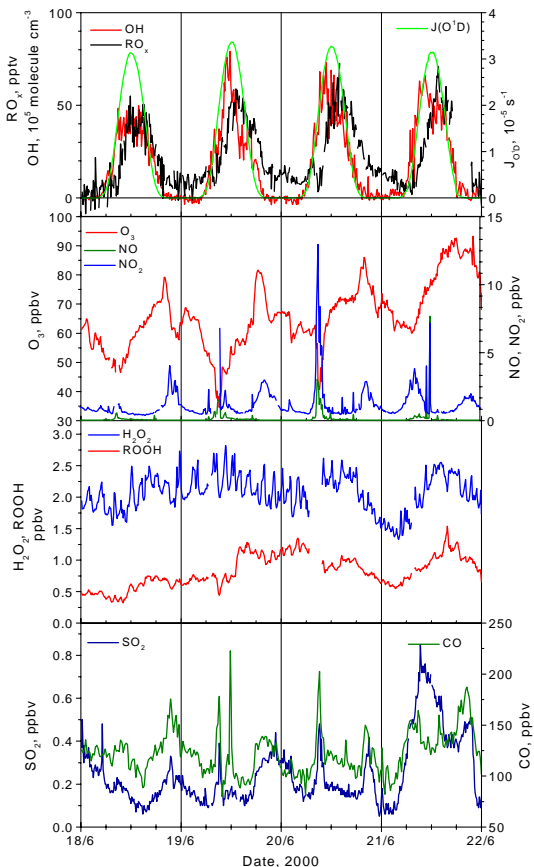


Fig. 2. Concentration of OH and mixing ratios of RO_x , ozone, NO, NO_2 , H_2O_2 , ROOH, CO and SO_2 measured at Hohenpeissenberg during the period 18 to 21 June, 2000. Data gaps are due to instrument calibration.

Title Page	
Abstract	Introduction
Conclusions	References
Tables	Figures
	
	
Back	Close
Full Screen / Esc	
Print Version	
Interactive Discussion	

Hohenpeissenberg Photochemistry Experiment

Handsides et al.

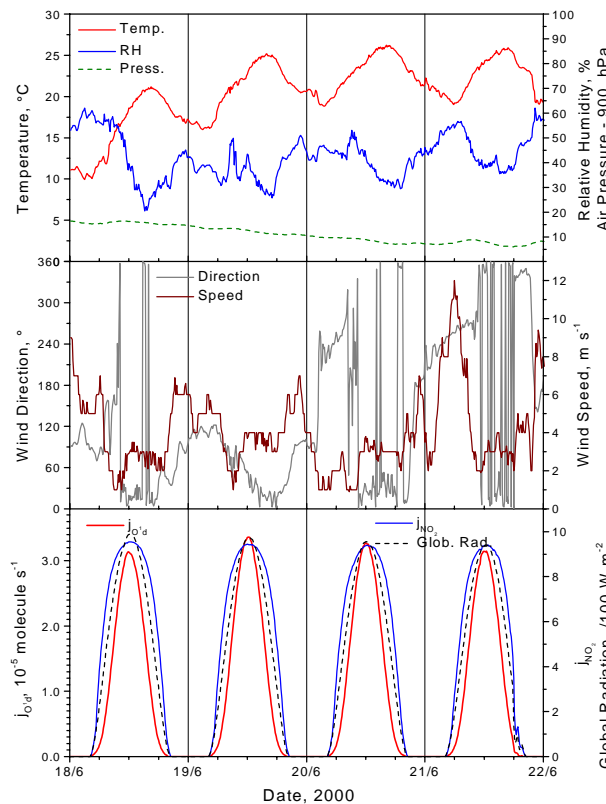


Fig. 3. Meteorological parameters at Hohenpeissenberg during the period 18 to 21 June, 2000.

Print Version

Interactive Discussion

© EGU 2002

**Hohenpeissenberg
Photochemistry
Experiment**

Handisides et al.

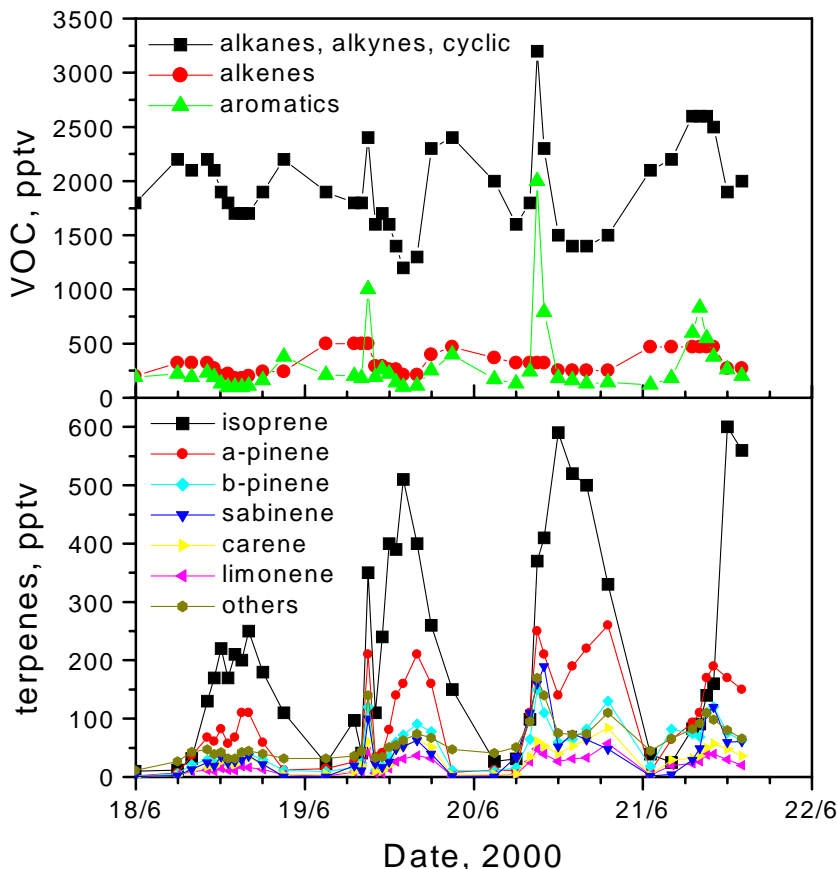


Fig. 4. Mixing ratios for various groups of NMHCs at Hohenpeissenberg during the period 18 to 21 June, 2000. The group labeled alkenes in the upper panel includes neither isoprene nor the terpenes.

[Title Page](#)

[Abstract](#)

[Introduction](#)

[Conclusions](#)

[References](#)

[Tables](#)

[Figures](#)

[◀](#)

[▶](#)

[◀](#)

[▶](#)

[Back](#)

[Close](#)

[Full Screen / Esc](#)

[Print Version](#)

[Interactive Discussion](#)

**Hohenpeissenberg
Photochemistry
Experiment**

Handisides et al.

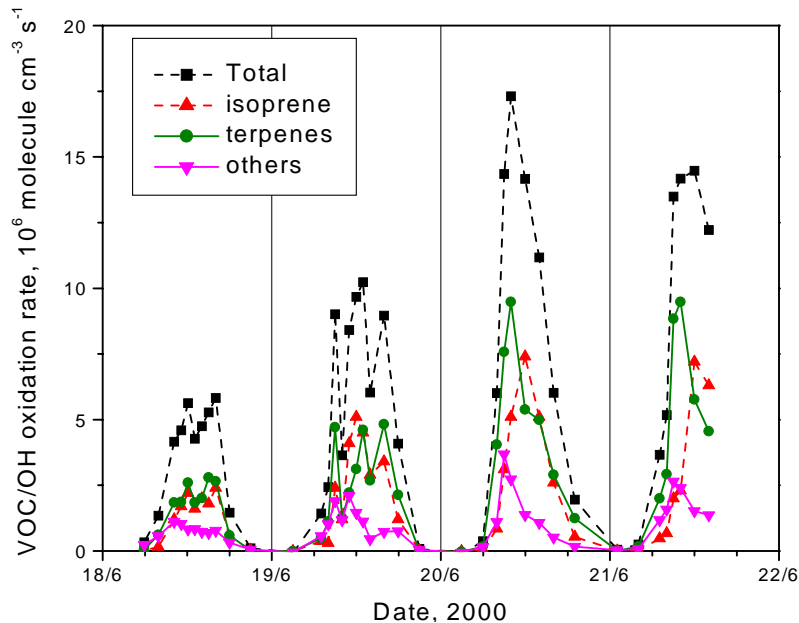


Fig. 5. Plot of the contributions of isoprene, terpenes, and the other NMHCs to the total oxidation rate of NMHC by OH.

[Title Page](#)[Abstract](#)[Introduction](#)[Conclusions](#)[References](#)[Tables](#)[Figures](#)[◀](#)[▶](#)[Back](#)[Close](#)[Full Screen / Esc](#)[Print Version](#)[Interactive Discussion](#)

Hohenpeissenberg Photochemistry Experiment

Handisides et al.

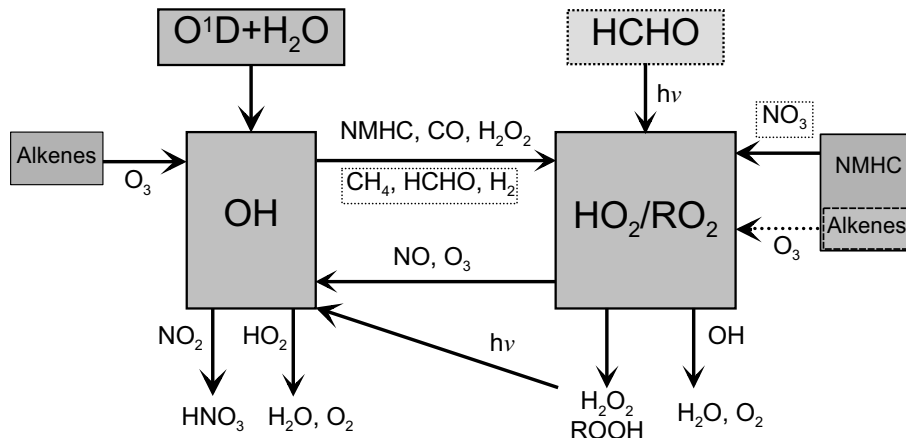


Fig. 6. Block diagram of the chemistry considered in the photostationary state calculations. Components whose concentrations were approximated are indicated by dashed boxes.

Title Page	
Abstract	Introduction
Conclusions	References
Tables	Figures
◀	▶
◀	▶
Back	Close
Full Screen / Esc	
Print Version	
Interactive Discussion	

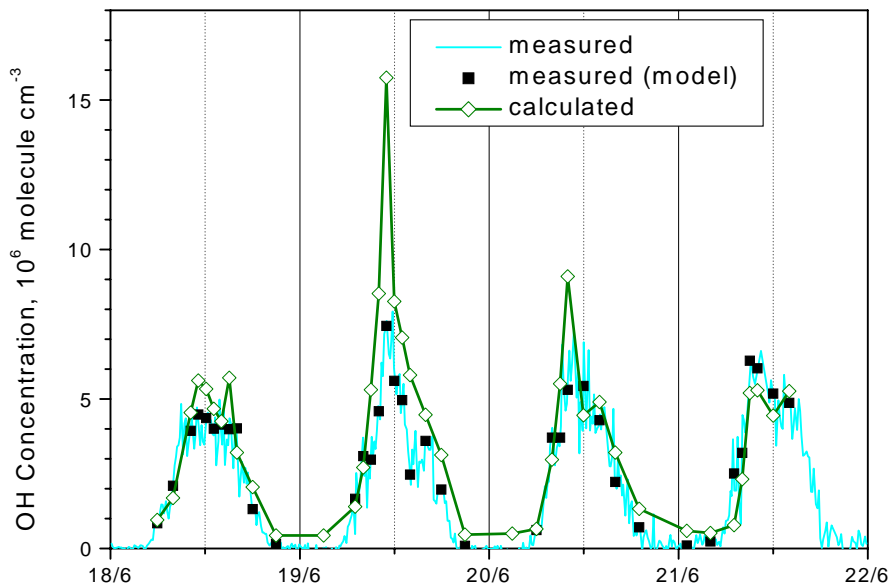


Fig. 7. Plot of the observed OH concentration and the concentration derived from photostationary state radical balance calculations for the period 18–21 June, 2000. The measured OH concentration is represented by the solid line. Observations corrected for inlet chemistry on the basis of NMHC measurements are shown as solid squares.

Hohenpeissenberg Photochemistry Experiment

Handisides et al.

[Title Page](#)

[Abstract](#)

[Introduction](#)

[Conclusions](#)

[References](#)

[Tables](#)

[Figures](#)

◀

▶

◀

▶

[Back](#)

[Close](#)

[Full Screen / Esc](#)

[Print Version](#)

[Interactive Discussion](#)

Hohenpeissenberg Photochemistry Experiment

Handisides et al.

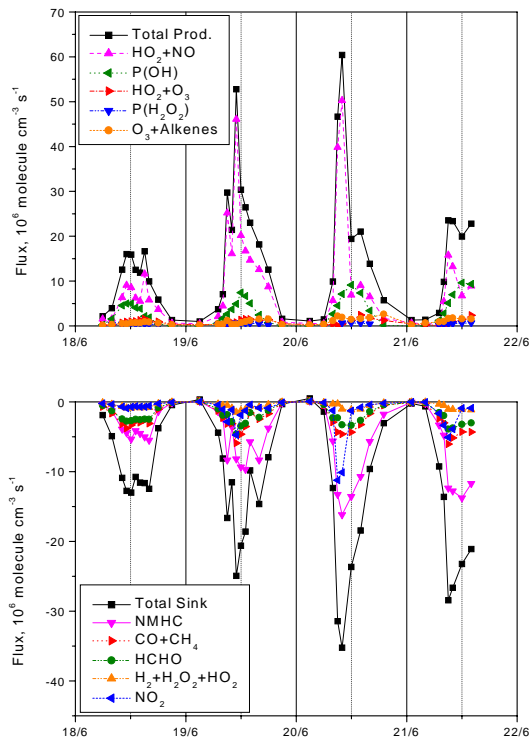


Fig. 8. Plot of the calculated contributions of various sources and sinks of OH for the period 18–21 June, 2000. The scales are different for the two panels.

[Title Page](#)

[Abstract](#)

[Introduction](#)

[Conclusions](#)

[References](#)

[Tables](#)

[Figures](#)

[◀](#)

[▶](#)

[◀](#)

[▶](#)

[Back](#)

[Close](#)

[Full Screen / Esc](#)

[Print Version](#)

[Interactive Discussion](#)

Hohenpeissenberg Photochemistry Experiment

Handisides et al.

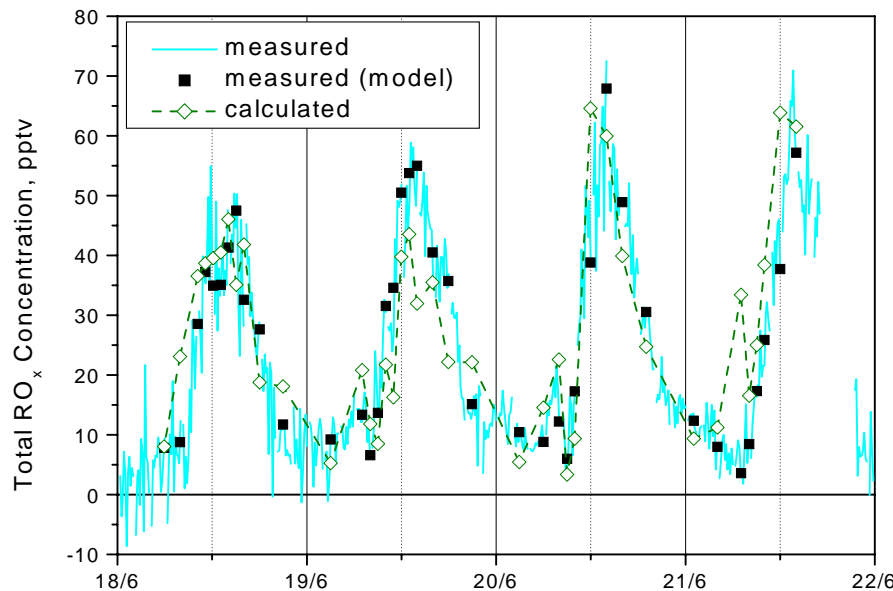


Fig. 9. Plot of the observed RO_x mixing ratio and the results of the photostationary state radical balance calculations for the period 18–22 June, 2000. Observations made at the time of the NMHC measurements are shown as solid squares.

Title Page	
Abstract	Introduction
Conclusions	References
Tables	Figures
	
	
Back	Close
Full Screen / Esc	
Print Version	
Interactive Discussion	

Hohenpeissenberg Photochemistry Experiment

Handisides et al.

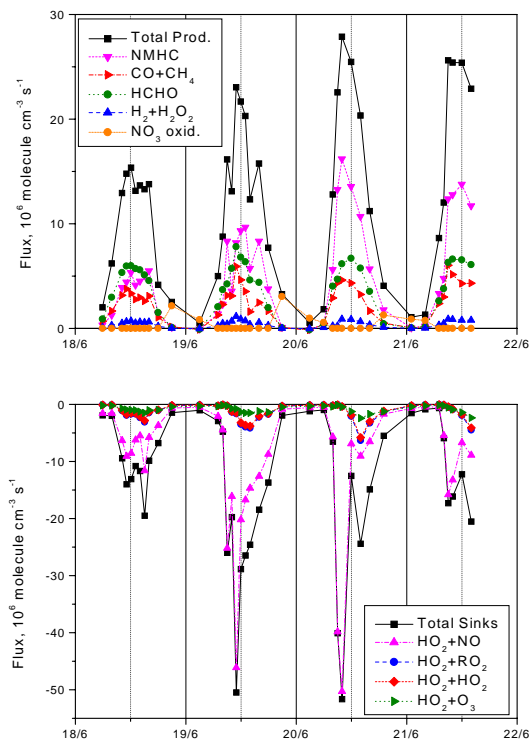


Fig. 10. Plot of the calculated contributions of various sources and sinks of RO_x for the period 18–21 June, 2000. The scales are different for the two panels. Sinks were calculated using the measured RO_x mixing ratios.

[Title Page](#)

[Abstract](#)

[Introduction](#)

[Conclusions](#)

[References](#)

[Tables](#)

[Figures](#)

[◀](#)

[▶](#)

[◀](#)

[▶](#)

[Back](#)

[Close](#)

[Full Screen / Esc](#)

[Print Version](#)

[Interactive Discussion](#)

Hohenpeissenberg Photochemistry Experiment

Handisides et al.

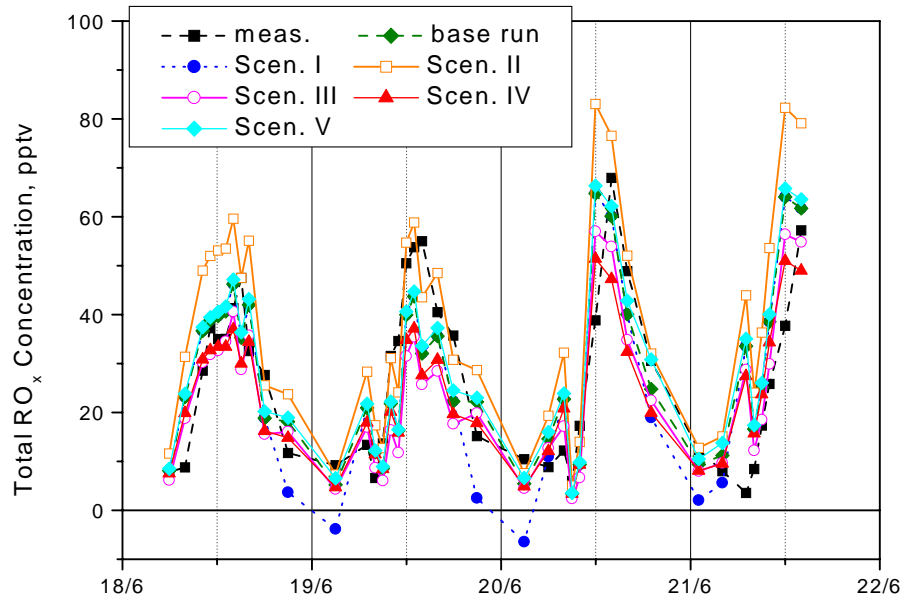


Fig. 11. Comparison of the RO_x mixing ratios obtained using the photostationary state radical model for the following scenarios. The scenarios are discussed in the text.

Base Run
Scenario I
Scenario II
Scenario III
Scenario IV
Scenario V

As in Fig. 9 with HCHO and NO₃ oxidation without NO₃ oxidation
with [HO₂]=[RO₂]/2
with only 50% conversion of RO₂ to HO₂
with reaction coefficients for R ≥ C₂
with 50% yield of RO₂ from ozonolysis of alkenes

Title Page	
Abstract	Introduction
Conclusions	References
Tables	Figures

◀	▶
◀	▶
Back	Close

Full Screen / Esc
Print Version
Interactive Discussion

**Hohenpeissenberg
Photochemistry
Experiment**

Handisides et al.

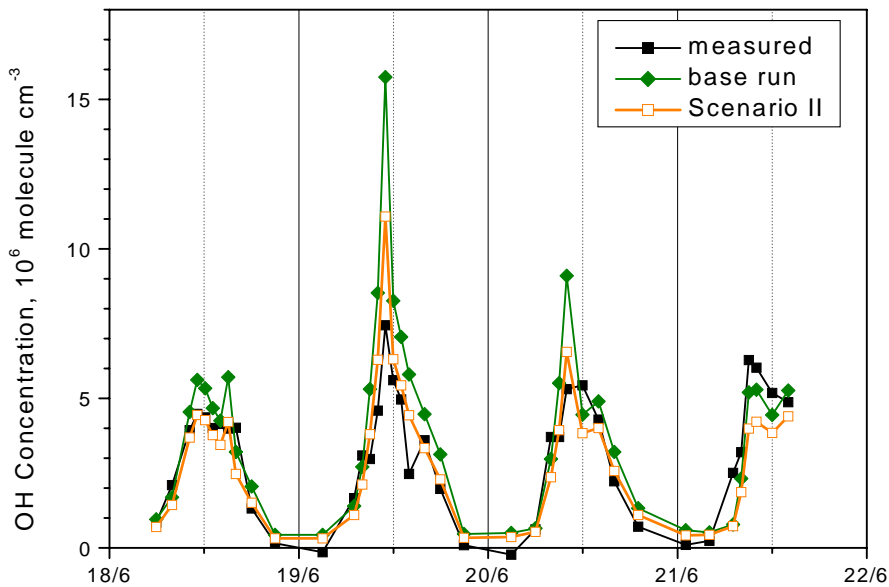


Fig. 12. Comparison of the OH concentration obtained using the photostationary state radical model for the base run and for Scenario II.

[Title Page](#)[Abstract](#)[Introduction](#)[Conclusions](#)[References](#)[Tables](#)[Figures](#)[◀](#)[▶](#)[◀](#)[▶](#)[Back](#)[Close](#)[Full Screen / Esc](#)[Print Version](#)[Interactive Discussion](#)